Journal of Mammalian Evolution (2021) 28:221–243
https://doi.org/10.1007/s10914-020-09520-x

ORIGINAL PAPER

The Skeleton of the Manus of *Scelidotherium* (Xenarthra, Mylodontidae) Specimens from the Pleistocene of the Province of Córdoba, Argentina, and its Systematic Implications

Gastón L. Nieto[1,2] · J. Augusto Haro[1,2] · H. Gregory McDonald[3] · Ángel R. Miño-Boilini[2,4] · Adan A. Tauber[1,5] · Jerónimo M. Krapovickas[1,5] · Maximiliano N. Fabianelli[1] · Federico M. Rosas[1]

Accepted: 20 September 2020 / Published online: 16 October 2020

Abstract

Dental and craniomandibular data have been predominantly used to infer relationships among mylodontid ground sloths. Recent studies indicate the osteology of the manus also provides useful data to test phylogenetic relationships in mylodontine mylodontids. Here we provide new comparative data from the study of the manus of a member of the Scelidotheriinae, *Scelidotherium* Owen, 1839, based on specimens from the Province of Córdoba that provide information on the variation and systematic relationships of the genus. The *Scelidotherium* material from the Province of Córdoba in central Argentina presents several morphological differences with material of the genus from northwestern Argentina. The manus of *Scelidotherium* shares several traits with *Catonyx* Ameghino, 1891, but not with *Valgipes* Gervais, 1874. These include: trapezoid with a sharp ridge on the articular surface for metacarpal II; magnum with at least half of articular surface for metacarpal II located on the dorsal half of the medial and distal aspects of the bone; metacarpal II with a notch on the axial border of its distal articular surface; and ungual process of the distal phalanx of the second digit markedly dorsopalmarly flattened. A phylogenetic analysis that includes osteological characters of the manus indicates that within the family Scelidotheriinae, *Scelidotherium* is more closely related to *Catonyx* than to *Valgipes* or *Proscelidodon gracillimus* Rovereto, 1914.

Keywords *Scelidotherium* · Manus · Phylogeny · Province of Córdoba

Introduction

The osteology of the South American sloth genus *Scelidotherium* Owen, 1839, is well known (e.g., Owen 1839, 1857; Burmeister 1881; Cuenca Anaya 1995), largely on the basis of very complete individuals belonging to the type species *Scelidotherium leptocephalum* Owen, 1839 (Burmeister 1881; Lydekker 1894; Cuenca Anaya 1995). The only other species undoubtedly assigned to this genus, *Scelidotherium parodii* Kraglievich, 1923, is known by less material, mostly restricted to the skull and humerus (Kraglievich 1923; McDonald 1987; Miño-Boilini 2012).

Electronic supplementary material The online version of this article (https://doi.org/10.1007/s10914-020-09520-x) contains supplementary material, which is available to authorized users.

✉ J. Augusto Haro
augustoharo@unc.edu.ar

[1] Departamento de Geología Básica, Facultad de Ciencias Exactas, Físicas y Naturales, Universidad Nacional de Córdoba, Vélez Sarsfield 1611, X5016GCA Córdoba, Province of Córdoba, Argentina

[2] Consejo Nacional de Investigaciones Científicas y Técnicas (CONICET), Godoy Cruz 2290, C1425FQB Ciudad Autónoma de Buenos Aires, Argentina

[3] Bureau of Land Management, Colorado State Office, 2850 Youngfield Street, Lakewood, CO 80215, USA

[4] Centro de Ecología Aplicada del Litoral, Consejo Nacional de Investigaciones Científicas y Técnicas (CONICET), Universidad Nacional del Nordeste (UNNE), Ruta 5. km, 2,5, 3400 Corrientes, Province of Corrientes, Argentina

[5] Museo Provincial de Ciencias Naturales "Dr. Arturo Umberto Illía", Poeta Lugones 395, X5000HZD Córdoba, Province of Córdoba, Argentina

These specimens have facilitated assessing the phylogenetic interrelationships of the species included in the genus with other scelidotheriines in a handful of published works (McDonald and Perea 2002; Cartelle et al. 2009; Corona 2012; Miño-Boilini 2012; Miño-Boilini et al. 2014). Among these different studies, the results of McDonald and Perea (2002) and Cartelle et al. (2009) are similar, but those of Miño-Boilini (2012) and Miño-Boilini et al. (2014) differ in their conclusions. A difference between these studies is the discrepancy concerning the closest relatives of *Scelidotherium* (including *Scelidotherium parodii*). In all of these studies the matrices are primarily based on cranial, mandibular, and dental characters. The data matrix in McDonald and Perea (2002) only presented two parsimony-informative postcranial characters out of a total of 22, and Miño-Boilini (2012) presented four parsimony-informative postcranial characters out of 21. Therefore, one way to resolve the incongruence between these studies may be the inclusion of more postcranial characters. A recent study (Haro et al. 2016) indicated that the skeleton of the manus provides useful characters for phylogenetic studies in mylodontine ground sloths. Due to the sister-group relationship of mylodontines to scelidotheriines (McDonald 1987; Gaudin 2004; Haro et al. 2016), the structure of the manus may also potentially provide parsimony-informative data to unravel the relationship of *Scelidotherium* to the other scelidotheriines.

The taxonomic usefulness of characters in the bones of the manus in this group is clear: previous systematic decisions, such as referring *S. leptocephalum* and *Catonyx cuvieri* (Lund, 1839a), but not *Valgipes bucklandi* (Lund, 1839b), to the genus *Scelidotherium*, is based largely on the structure of the manus (Winge 1915). Furthermore, previous studies have proposed characters from the manus as diagnostic features of *Scelidotherium* or the species *S. leptocephalum*, including the absence of an ungual in the pollex and the reduction of the contact between the unciform and metacarpal V (Schulthess 1920; McDonald 1987). Despite the existence of several descriptions of the bones of the hand of *Scelidotherium* (e.g., Burmeister 1881; Schulthess 1920; McDonald 1987; Esteban et al. 1992; Cuenca Anaya 1995), and comparative information of hand structure that may inform phylogenetic analysis (e.g., Winge 1915; Ortega 1967; McDonald 1987), this skeletal region has not yet been fully examined to detect characters useful to determine the relationships of *Scelidotherium* with other scelidotheriines.

Recognition of variation is also important in dealing with the phylogenetic relationships of a taxon (Boscaini et al. 2019). Comparative studies of morphology of specimens from different regions or ages that belong to the same species are more likely to increase our knowledge of intraspecific variation than comparisons of specimens from the same region or age, because regional and temporal variation is added to random or sexual variation. For example, McDonald (1987) indicated there is size variation between *S. leptocephalum* specimens of different age. The latter author also considered there is some evidence suggesting geographical variation in body size for *Catonyx chiliense* (Lydekker, 1886). Another example is a study of *C. cuvieri* from Uruguay, which increased our knowledge of its variation, which overlaps that of *Scelidotherium* in certain features (Corona et al. 2013). Most previous descriptions of the manus of *Scelidotherium* deal with specimens from the Pampean Region of Argentina (e.g., Burmeister 1881; Schulthess 1920; McDonald 1987; Cuenca Anaya 1995), but Esteban et al. (1992) described the manus of *S. leptocephalum* from the Province of Salta in northwestern Argentina. A problem is that the lack of detailed specimen-based descriptions (with explicit provenances for the specimens) in the previous literature precludes identifying geographical variations even if intraspecific differences are described in mani of *Scelidotherium*.

Hoping to contribute knowledge useful to resolve these problems related to systematics, here we describe bones from scelidotheriine hands from three different individuals collected from the late Pleistocene of the Province of Córdoba, in central Argentina, intermediate in location between the aforementioned specimens of *Scelidotherium*. Haro et al. (2016) referred all of these to *Scelidotherium*, on the basis of the lack of contact between metacarpal V and the unciform. One of these, previously referred to the species *S. leptocephalum* (Krapovickas et al. 2017), represents a remarkably complete manus. However, considering that some specimens of *C. cuvieri* also lack contact between metacarpal V and the unciform (Winge 1915), the basis for such referral is insufficient. In this work we test the referral of the specimens from the Province of Córdoba to the genus *Scelidotherium*, and document the implications of the characters from the manus of that material to the study of variation and phylogenetic interrelationships of that taxon among the Scelidotheriinae.

Materials and Methods

The studied materials belong to three specimens. CORD PZ 4464 is an articulated complete left thoracic member (i.e., forelimb). CORD PZ 4586 includes a partially preserved left manus, including scaphoid, lunar, cuneiform, co-ossified trapezoid and magnum, unciform, co-ossified trapezium and metacarpal I, metacarpals II and IV, proximal phalanx of digit I, ungual phalanx of digit II, and all phalanges of digit III. It is associated with the caudal part of the skull, a third metatarsal, other thoracic limb bones, and a few other unprepared bones. CORD PZ 11293 consists of an ulna, magnum, unciform, and many rib fragments.

Anatomical terminology follows the conventions of the Nomina Anatomica Veterinaria (International Committee on Veterinary Gross Anatomical Nomenclature 2005), in

agreement with Harris (2004). We follow the phylogenetic definitions of the Mylodontinae Gill, 1872, and the Scelidotheriinae Ameghino, 1904, proposed in Haro et al. (2016). Here we propose further phylogenetic definitions for Mylodontidae Gill, 1872, and Mylodontoidea Gill, 1872. We define Mylodontidae as the least inclusive node-based clade including *Mylodon darwinii* Owen, 1839, *Scelidotherium leptocephalum* Owen, 1839, their common ancestor, and all its descendants. We define Mylodontoidea as the stem-based clade encompassing all taxa more closely related to *M. darwinii* than to *Megatherium americanum* Cuvier, 1796, and *Megalonyx jeffersonii* Desmarest, 1822.

Comparisons were made principally with other members of the Scelidotheriinae. These comparisons based on traits noted in descriptions of the manus in the scelidotheriine taxa listed in Table 1. Further comparisons are made with the specimen PVUNS 198, referred to *Proscelidodon* Bordas, 1935, by Aramayo (1988) and to *Scelidotherium* by Esteban et al. (1992). We assembled those comparisons into character-taxon matrices (Supplementary Data S1–S4) containing 177 characters (Supplementary Data S5), of which 24 belong to the skeleton of the manus. A few characters from the manus are continuous, and are treated as such (sensu Goloboff et al. 2006). Because of the error of scaling based on total range of values for a character (Farris 1990), each continuous character is scaled so that the mean weight of all its parsimony-informative transformations equals one (the procedure is explained and justified in Supplementary Data S5). The characters are based on the studies of Winge (1915), Kraglievich (1923), Ortega (1967), McDonald (1987), Scillato-Yané and Carlini (1998), McDonald and Perea (2002), Gaudin (2004), and Miño-Boilini (2012), and also include new ones proposed in this study. Only those characters that are parsimony-informative for the sampled taxa were included. Winge (1915) provided most of the manus traits we have included. Among characters provided by Gaudin (2004), all those being parsimony-informative for the included taxa were included. Incorporation of characters in Gaudin (2004) was used instead of constraints to recover the relative position of the included outgroups (whose interrelationships are not the focus of our work) supported by large morphology-based analyses (i.e., Gaudin 2004; Boscaini et al. 2019).

We performed a phylogenetic analysis including all characters, using the presently described specimens as independent terminals (Analysis 1), in order to test their referral to the genus *Scelidotherium*. Use of the criterion of parsimony with specimens as independent terminals in phylogenetic analyses informs alpha-taxonomic assignments (Vrana and Wheeler 1992; Yates 2003; Tschopp et al. 2015). On the grounds of parsimony, the hypothesis of referral to the genus *Scelidotherium* can be rejected if the specimens are not recovered most closely related to species of *Scelidotherium* than to other species. Reference to the species *S. leptocephalum* would be only possible if, unlike in previous analyses, the genus turns out to be not monophyletic, because the only other undisputed species of *Scelidotherium*, *S. parodii*, is mostly known by the facial region of the skull (Kraglievich 1923), which is lacking in the specimens here reported. We performed a second analysis, in which we combined all the information from *S. leptocephalum*, *S. parodii*, and all the specimens more closely related to these than to species of genera different from *Scelidotherium* (according to the results of the previous analysis), within a single terminal representing the genus *Scelidotherium* (Analysis 2). This analysis, incorporating the data from the presently described specimens within a taxon, would better inform on the relationships of that taxon. For the sake of comparison with the complete dataset, we performed two other phylogenetic analyses using the same

Table 1 Taxa and material used for comparisons. Collection numbers refer to specimens studied first hand. Bibliographical citations on the right column are sources of descriptions

Taxon	Material used for comparisons
Scelidotherium leptocephalum Owen, 1839	Burmeister (1881); Winge (1915); Schulthess (1920); Ortega (1967); McDonald (1987); Esteban et al. (1992); Cuenca Anaya (1995)
Catonyx chiliense (Lydekker, 1886)	Sefve (1915); McDonald (1987)
Catonyx tarijensis (Gervais and Ameghino, 1880)	McDonald (1987)
Catonyx cuvieri (Lund, 1839a)	Lund (1839a, 1842); Winge (1915); Schulthess (1920); McDonald (1987); Cartelle et al. (2009)
Valgipes bucklandi (Lund, 1839b)	Winge (1915); Cartelle et al. (2009)
Proscelidodon gracillimus (Rovereto, 1914)	Ortega (1967); McDonald (1987)
Proscelidodon patrius (Ameghino, 1888)	McDonald (1987)
Mylodon darwinii Owen, 1839	CORD PZ 4570; Haro et al. (2016); McAfee (2016)
Pseudoprepotherium confusum Hirschfeld, 1985	Hirschfeld (1985)
Hapalops longiceps Scott, 1904	Scott (1904)
Choloepus Illiger, 1811	*Choloepus hoffmanni* Peters, 1858 specimens: DMNS 2654, 2656, 2657, 6458; Anthony (1909)
Nematherium Ameghino, 1887	Scott (1904)

terminals as the previous one: one only including the characters belonging to the manus (Analysis 3) and one including all characters except for those of the manus (Analysis 4).

The data matrix was assembled using Microsoft Excel 2013. We performed the phylogenetic analyses with the program TNT (Goloboff et al. 2003; Goloboff and Catalano 2016). The analyses were based on equal-weights parsimony and searches were exact. No aprioristic constraints were used. We used the 'Pruned trees' command in TNT to identify wildcard terminals once the analysis was performed. This identification was used to hide such terminals from the strict consensus, in order to detect resolution hidden by their presence. No analyses were run excluding wildcard terminals. We obtained the strict consensus and the reduced strict consensus trees. We calculated jackknife frequencies (p: 0.36; 10,000 replicates) and Bremer support values on the strict consensus trees. We only used unambiguous optimization for reconstruction of the character state evolution because TNT does not provide ACCTRAN or DELTRAN reconstructions.

The ingroup includes all of the scelidotheriines included in the comparisons indicated above plus *S. parodii*, *Procelidodon rothi* (Ameghino, 1908), and *Sibyllotherium guenguelianum* Scillato-Yané and Carlini, 1998. The present taxon list includes as terminals those specimens here described, as well as the one studied in Aramayo (1988), PVUNS 198, to test its referral to *Scelidotherium* by Esteban et al. (1992). The choice of the ingroup terminals was made attempting to include all possible scelidotheriine taxa. This implies including the terminals used by previous phylogenetic works (McDonald and Perea 2002; Cartelle et al. 2009; Miño-Boilini 2012) and manual material of uncertain affiliation (Aramayo 1988). We selected five sloth taxa as outgroups based on a previous large phylogenetic study (Gaudin 2004), and did not enforce outgroup topology a priori. These five taxa are *M. darwinii*, *Pseudoprepotherium confusum* Hirschfeld, 1985, *Hapalops longiceps* Scott, 1904, the extant genus *Choloepus* Illiger, 1811, and the more incompletely known genus *Nematherium* Ameghino, 1887. Use of the genus *Nematherium* as outgroup follows its usage in previous phylogenetic studies of scelidotheriines (e.g., McDonald and Perea 2002; Miño-Boilini 2012). The selection of *Ps. confusum* and *H. longiceps* as outgroups was based on their currently accepted status as early representatives of mylodontines and megatherians, respectively, for which several bones of the hand skeleton are known and described (Scott 1904; Hirschfeld 1985). The selection of *M. darwinii* as a further outgroup is based on both the amount of data on the structure of the manus available, and comparatively studied (Haro et al. 2016), and its status as a member of the Mylodontinae, the closest relatives to scelidotheriines (according to Gaudin 2004). The selection of the genus *Choloepus* as a further outgroup is based on its recognition as a mylodontoid in recent molecular analyses (Delsuc et al. 2019; Presslee et al. 2019). Source data are available in Table 1.

Availability of Data and Material All data generated or analyzed during this study are included in this published article [and its supplementary information files].

Institutional Abbreviations: **CORD PZ**, Colección de Paleozoología, Museo de Paleontología, Universidad Nacional de Córdoba, Córdoba, Argentina; **DMNS**, Denver Museum of Nature and Science, Colorado, U.S.A.; **PMU**, Paleontologiska Museet Uppsala Universitet, Uppsala, Sweden; **PVUNS**, Paleontología de Vertebrados, Universidad Nacional del Sur, Bahía Blanca, Argentina; **ZMK 1/1845** (previously referred to ZMUC), Lund's collection, Zoologisk Museum, Statens Naturistoriske Museum, Københavns Universitet, Copenhagen, Denmark.

Systematic Paleontology

Tardigrada Latham and Davies, 1795
Mylodontidae Gill, 1872
Scelidotheriinae Ameghino, 1904

Scelidotherium Owen, 1839

Type Species *Scelidotherium leptocephalum* Owen, 1839, from Punta Alta, Bahía Blanca, Province of Buenos Aires, Argentina.

Included Species The species *Scelidotherium leptocephalum*, the youngest and largest species in body size, was distinguished from *Scelidotherium bravardi* Lydekker, 1886, by Lydekker (1886) and more recently by Miño-Boilini et al. (2014), and from *Scelidotherium parodii* by Kraglievich (1923). McDonald (1987) considered *S. bravardi* a junior synonym of *S. leptocephalum* and that the slight difference in size reflects its older age as there is a trend for the species to increase through time.

Diagnosis The following diagnosis is based on McDonald (1987), with additions from Miño-Boilini et al. (2014). Skull elongate, narrow; nasal passage narrower than in *Catonyx* Ameghino, 1891, or *Proscelidodon*, and not inflated. Dorsal profile of braincase flat, lacking concavity of *Catonyx* or dorsal swellings of *Proscelidodon*. Occiput sloped posteroventrally with occipital condyles projecting posteriorly. Temporal cristae parallel and not diverging to the supraorbital processes until anterior of frontoparietal suture (usually approximately level with postorbital constriction); no sagittal crest. Dorsal inclination of predental part of maxilla weak, 0 to 10° relative to the tooth-bearing part of the maxilla. Ventral portion of maxilla between toothrows straight, lacking median

grooves. Premaxilla with constant dorsoventral thickness (not tapering rostrally as in *Catonyx* and *Proscelidodon*), lacking step for contact with the anterior edge of the premaxillary process of the maxilla. Lateral process of nasal extends anteriorly beyond the edge of the maxilla. Paroccipital process mediolaterally flattened and projecting ventrally to the entotympanic. Tympanohyal with posterior expansion between mastoid and paroccipital processes. Teeth small in proportion to size of the skull compared to *Catonyx* and *Proscelidodon*. First upper tooth narrower relative to length than in *Catonyx*. Second to fourth upper teeth forming elongated triangles lacking buccal furrows, corners not forming distinct lobes in occlusal aspect. Mandibular symphysis forming an elongated spout, squared anteriorly and flattened; internal surface shallow; angle of spout to tooth row small, average 17°; symphysis lacking ventral keel. Posterior lobe of lower fourth tooth parallel to anterior lobe and without lingual curve. Digit I of manus reduced and without ungual phalanx. Scaphoid with proximal and distal articular surfaces well separated on the dorsum. Metacarpal IV with articular facets for metatarsal III and unciform that meet at an obtuse angle. Femur relatively short with a strong medial slope of the proximal end relative to the distal end; medial surface of femoral shaft concave.

Scelidotherium sp.

Referred Material Materials listed in McDonald (1987) and Miño-Boilini et al. (2014), as well as specimens CORD PZ 4586, 4464, and 11293.

Hypodigm Specimens CORD PZ 4586, 4464, and 11293.

Localities and Horizons CORD PZ 4464 was collected in Pampa de Oláen (Province of Córdoba), Vaca Corral Formation, late Pleistocene (Lujanian SALMA) (31°9′11.2”S; 64°35′31.3”W; 1138 m.a.s.l.; Krapovickas et al. 2017). CORD PZ 4586 comes from the vicinity of Noetinger, on the Pampean plains, age is uncertain, unattributed loess deposits (Leguizamón et al. 2000). CORD PZ 11293 was collected in Sierra de Las Peñas (32°34′39”S, 64°20′14”W), east of the nearby town of Elena, Province of Córdoba (Fig. 1), La Invernada Formation, late Pleistocene (Lujanian SALMA).

Description

The following description focuses on characters showing variation among scelidotheriines. Measurements are provided in Table 2 and Supplementary Data S5 (Tables S2 to S5). In CORD PZ 4464 carbonate concretions make it difficult to disarticulate most bones in order to describe the articular surfaces (Fig. 2) or obtain measurements.

Brief Notes on the Non-manual Skeleton

The skull of CORD PZ 4586 presents temporal lines quite separate from the midline, caudal borders of the temporal fossae not parallel to the borders of the occiput, a trough between the paroccipital and mastoid processes obstructed by the tympanohyal, and well-developed fossae for the *M. rectus* capitis ventralis on the basioccipital. All these features are shared with *Scelidotherium*, but not *Catonyx* (McDonald 1987). The humerus of CORD PZ 4464 presents an entepicondylar foramen, as in *S. leptocephalum* and most other scelidotheriines, but not *Catonyx cuvieri* (Winge 1915). The radius of CORD PZ 4464 presents a prominent pronator crest of the radius, as in *S. leptocephalum*, but not *C. cuvieri* (Winge 1915). The ulna of CORD PZ 4464 and 11293 presents a relatively narrow proximocranial projection of the olecranon and an anconeal process of the ulna that is relatively not prominent, as in *S. leptocephalum*, but not *C. cuvieri* (Winge 1915). The ulna in both specimens presents a relatively blunt coronoid process, as in *S. leptocephalum*, but not *Catonyx tarijensis* Gervais and Ameghino, 1880, (Miño-Boilini 2016).

Carpus

Scaphoid CORD PZ 4586 presents a clearly distinct non-articular interval on the dorsal aspect that separates the proximal from distal articular surfaces. This is similar to some other *Scelidotherium* and *Valgipes* Gervais, 1874, specimens in ZMK 1/1845 (Winge 1915), but dissimilar to *C. chiliense* (PMU M4394; Sefve 1915) or the *C. cuvieri* material in ZMK 1/1845 (Winge 1915) in which the articular surfaces are much closer to one another or in contact. The medial part of the proximal articular surface presents a dorsopalmarly oriented concavity. The palmar border of the articular surface for the radius is just a little less distally extended on the palmar surface than the dorsal border is on the dorsal surface. In both CORD PZ 4464 and 4586 the scaphoid contacts the lunar by two surfaces completely separated by a recessed non-articular surface. This surface is proximodistally wide, and the facets are proximodistally narrow and dorsopalmarly elongate. The laterally facing proximal articular facet for the lunar, which contacts the articular surface for the radius at an edge, is slightly convex dorsopalmarly and straight proximodistally, and more closely resembles the condition of *C. cuvieri* than that of *V. bucklandi* described by Winge (1915). In both CORD PZ 4464 and 4586 the distal articular surface for the lunar contacts the articular surface for the magnum. In CORD PZ 4586 the distal articular surface for the lunar is flat, but in CORD PZ 4464 it is dorsopalmarly sinuous. The dorsopalmar

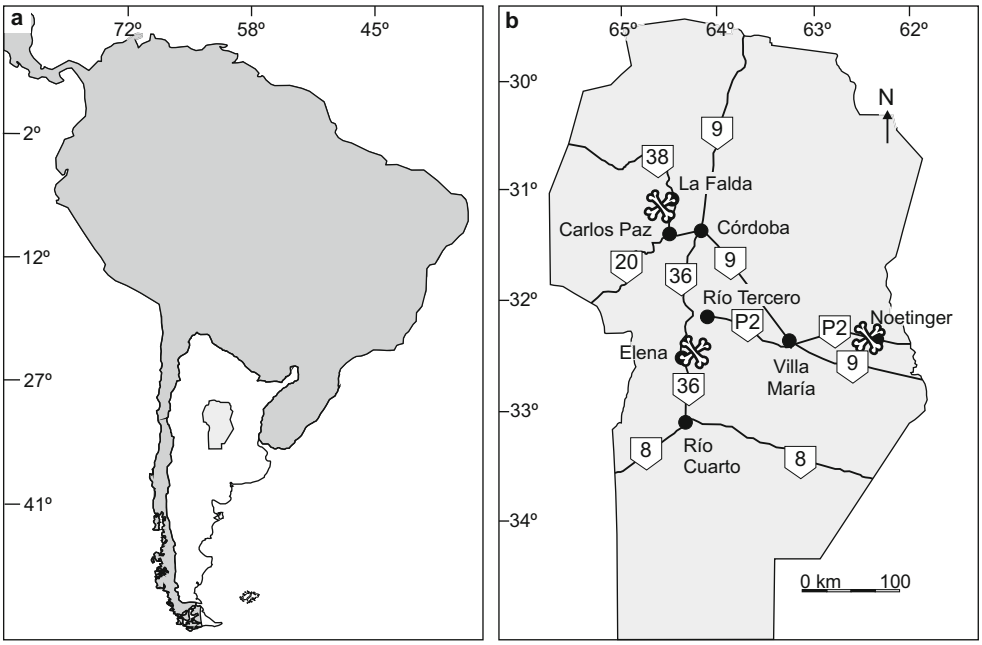

Fig. 1 Maps indicating provenances of the *Scelidotherium* Owen, 1839, specimens CORD PZ 4464, 4586, and 11293 from the Province of Córdoba, Argentina: **a**, map of South America (dark grey) indicating placement of the Province of Córdoba (light gray) within Argentina (white); **b**, close-up on the Province of Córdoba. Black dots in **b** represent urban centers, pentagons with numbers within represent highway routes, crossed-bone symbol indicates the location of the materials

depth of the bone at its lateral side, relative to its mediolateral breadth, is much higher than in the specimens of *S. leptocephalum*, *C. cuvieri*, and *V. bucklandi* measured by Winge (1915), although it more nearly approaches the specimens of the first species (Table 2). In CORD PZ 4464, in distal view, the long axis of the trapezial process is oblique relative to the lateral border of the articular facet for the magnum. The articular surface for the trapezium-metacarpal I is not clearly preserved. The subtriangular trapezoid articular facet presents a well-developed palmar angle, which in CORD PZ 4586 reaches the palmar half of the distal surface. In both CORD PZ 4464 and 4586, the articular facet for the magnum is single, as in *C. chiliense* and *C. cuvieri* (Sefve 1915; Winge 1915). This contrasts with the subdivided condition found in *V. bucklandi* (Winge 1915). In both CORD PZ 4464 and 4586, the articular surface is deeply concave and elongate in the dorsopalmar direction. It narrows mediolaterally at mid-length due to the presence of a notch in the medial border. This gives the facet a bilobate shape, with the palmar lobe mediolaterally wider. In CORD PZ 4586 (Fig. 3a), the lateral border of the articular facet for the magnum is straight. By contrast, in CORD PZ 4464 (Fig. 3b) that magnum facet border is sinuous and has a dorsal concavity and palmar convexity.

Lunar In both CORD PZ 4464 and 4586 the articular surfaces for the radius and cuneiform do not meet, unlike in *Proscelidodon gracillimus* Rovereto, 1914 (Ortega 1967). In CORD PZ 4586, the articular surface for the cuneiform forms an acute angle with the radial articular surface, in contrast to the straight angle present in *Pr. gracillimus* (Ortega 1967). Thus, the articular facet faces laterodistally. In CORD PZ 4586 the scaphoid articular facets do not occupy the entire dorsal border in medial aspect. This contrasts with the more extensive facet in *Pr. gracillimus* (McDonald 1987). In CORD PZ 4586, the proximal and distal articular surfaces for the scaphoid are continuous with the articular surfaces for the radius and the magnum, respectively. In CORD PZ

Table 2 Phylogenetically useful measurements (in millimeters) of hand bones of scelidotheriine specimens from the Province of Córdoba

Measurements	CORD PZ 4464	CORD PZ 4586
Greatest mediolateral width of scaphoid.	57.95	≥ 56.4
Greatest dorsopalmar depth of scaphoid at lateral side.	51.1	50.35
Greatest mediolateral width of trapezoid.	38	38.7
Maximum dorsopalmar depth of trapezoid.	39.4	42.6
Maximum proximodistal height of trapezoid on the medial side.	≥ 12.7	11.7
Maximum proximodistal length of metacarpal II.	–	82.5
Maximum axioabaxial width of metacarpal II at proximal end.	–	55.2

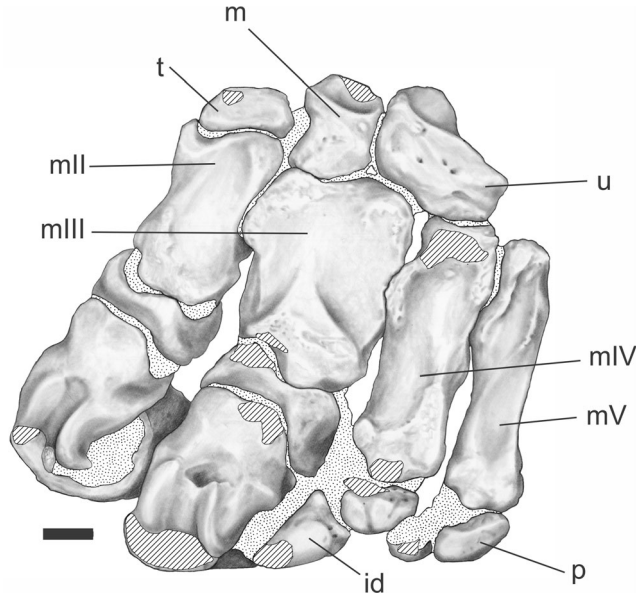

Fig. 2 Articulated block containing most bones of the manus (without the proximal carpal row) of the *Scelidotherium* Owen, 1839, specimen CORD PZ 4464 in dorsal view. *Abbreviations: id*, intermediate and/or distal phalanx of digit IV; *m*, magnum; *mII–V*, metacarpals II–V; *p*, proximal phalanx of digit V; *t*, trapezoid; *u*, unciform. Stippled areas represent sedimentary matrix; hatched areas represent breakage. Scale bar represents 20 mm

4586, the proximal part of the articular surface for the scaphoid is dorsopalmarly slightly concave and proximodistally roughly straight. In CORD PZ 4586, the dorsal part of the articular surface for the magnum presents a dorsopalmarly directed convexity (Fig. 3c), as in the *S. leptocephalum* specimen from Rosario de La Frontera (Esteban et al. 1992), and *C. cuvieri*, but in contrast with the thoroughly concave condition in *V. bucklandi* (Winge 1915). This convexity relates to the presence of a prominent oblique ridge within the surface (Winge 1915), which is lacking in *Pr. gracillimus* (Ortega 1967). The ridge is closer to the dorsal border than to the palmar one, as in *C. cuvieri* (Winge 1915), in contrast to the ridge closer to the palmar border reported in unspecified '*Scelidotherium*' materials by Ortega (1967). In CORD PZ 4586, the dorsal border of the articular surface for the magnum is wider than the palmar one, as in the scelidotheriine material studied by Cuenca Anaya (1995) and in *Pr. gracillimus* (Ortega 1967), but in contrast to the condition of unspecified '*Scelidotherium*' materials reported by Ortega (1967). In CORD PZ 4586, the articular surface for the unciform is dorsopalmarly extensive, reaching the dorsal border of the distal surface. This contrasts with the palmarly restricted condition of *V. bucklandi* (Winge 1915).

Cuneiform In CORD PZ 4586, the cuneiform's lateral side is proximodistally higher relative to the ulnar facet width (ratio: 0.98; Supplementary Data S5, Table S2). The ratio is included within the range of proportions of *C. cuvieri* (range of ratio: 0.83–1) but not in the range of other specimens of *Scelidotherium* (range of ratio: 0.78–0.83), and very far from those of *V. bucklandi* (range of ratio: 0.5–0.63), according to

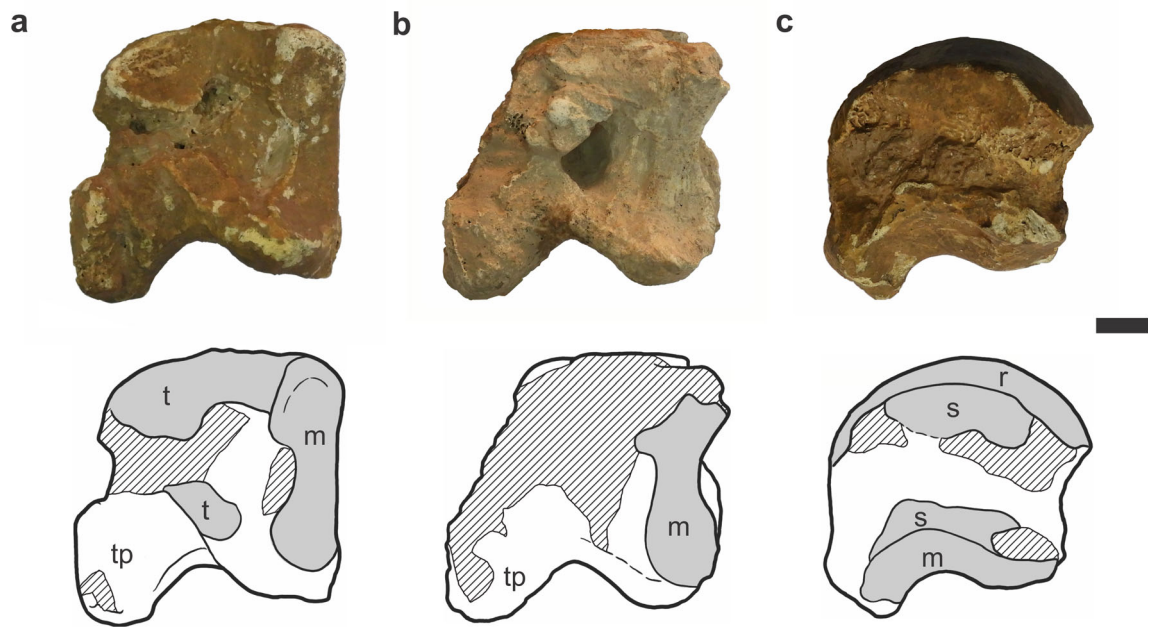

Fig. 3 Scaphoid and lunar of the *Scelidotherium* Owen, 1839, specimens CORD PZ 4586 and 4464. **a**, distal view of scaphoid in CORD PZ 4586; **b**, distal view of scaphoid in CORD PZ 4464; **c**, proximomedial view of lunar in CORD PZ 4586. *Abbreviations: m*, articular surface for magnum; *r*, articular surface for radius; *t*, articular surface for trapezoid; *s*, articular surface for scaphoid; *tp*, trapezial process. Each interpretative drawing is just below the corresponding photograph. On interpretative drawings, grey areas represent articular surfaces; hatched areas represent breakage. Scale bar equals 10 mm

measurements in Winge (1915). In CORD PZ 4464 and 4586, the ulnar articular surface is subtriangular (Fig. 4a, b), unlike the subcircular facet found in the *S. leptocephalum* specimen from Rosario de La Frontera (Esteban et al. 1992). The ulnar facet is more elongate in CORD PZ 4586 than in CORD PZ 4464. In CORD PZ 4464, the proximal articular surface extends a little into the medial side of the bone (Fig. 4c), as in the scelidotheriine material described by Cuenca Anaya (1995) and probably Esteban et al. (1992), if their 'articular surface for the radius' corresponds to this extension. On the other hand, in CORD PZ 4586 such an extension is absent (Fig. 4d). In CORD PZ 4586, the articular surface for the ulna is nearly flat, as in *C. cuvieri* (Lund 1842) and the *Scelidotherium* specimen from Rosario de La Frontera (Esteban et al. 1992) and PVUNS 198 (Aramayo 1988). On the other hand, in CORD PZ 4464 the surface is slightly convex along all axes, even without considering its medial extension. In both CORD PZ 4586 and CORD PZ 4464 the articular surface for the pisiform is largely flat, except for its proximodistally convex proximal region. In CORD PZ 4586, the articular surface for the pisiform is continuous with that for the ulna. By contrast, in CORD PZ 4464 it is partially separated by a rough surface. Both articular surfaces may be connected or not in *C. cuvieri* (Winge 1915). In CORD PZ 4464, the articular surface for the pisiform is elliptical in outline (Fig. 4e), unlike the subcircular facet of the *S. leptocephalum* specimen from Rosario de La Frontera (Esteban et al. 1992). In CORD PZ 4586, the outline of the facet has a subcircular main part (Fig. 4f) and a smaller, parallelogram-shaped part proximally that connects the subcircular part of the pisiform facet with the ulnar facet. CORD PZ 4586 bears a curved ridge medial to the pisiform facet whose position, orientation, and curvature resemble part of the pisiform facet border in CORD PZ 4464 (Fig. 4e, f). In CORD PZ 4586, this ridge, together with the border of the pisiform facet, limits an area very similar in shape to that occupied by the pisiform facet in CORD PZ 4464. The articular surface for the lunar contacts the articular surface for the unciform. In CORD PZ 4464 and 4586, the medial part of the articular surface for the unciform is saddle-shaped, with a dorsopalmar convexity and a mediolateral concavity, unlike the concave facet of *V. bucklandi* (Winge 1915). In CORD PZ 4464, the lateral part is slightly mediolaterally concave, but in CORD PZ 4586 it is slightly mediolaterally convex.

Pisiform It is walnut-shaped. The relatively large articular surface for the cuneiform is adjacent to but separated by an obtuse edge from the relatively small articular surface for the ulna. The cuneiform facet is concave on the direction of the lesser axis, but mostly straight along the direction of the major axis. A concavity is also present in this facet in other scelidotheriines (Winge 1915; McDonald 1987; Cuenca Anaya 1995).

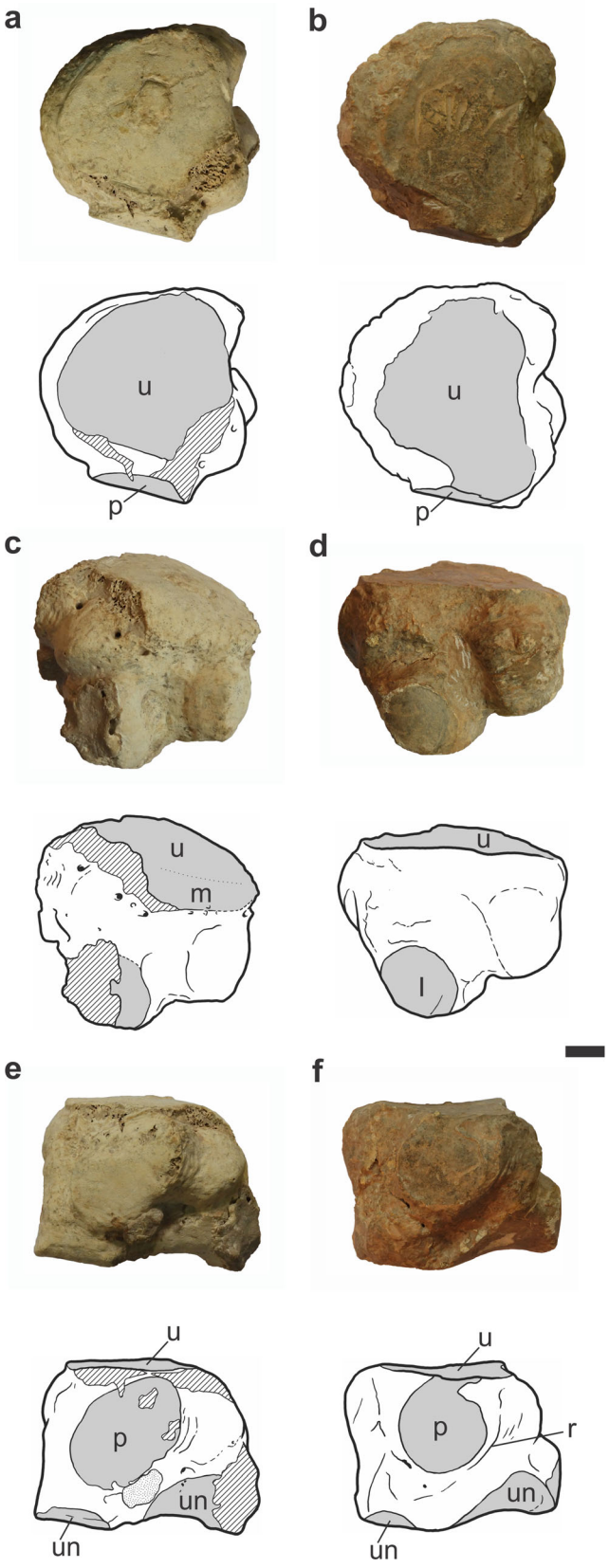

Trapezoid In CORD PZ 4586, the trapezoid is fused with the magnum (Fig. 5a–f), as in the *C. cuvieri* specimen ZMK

◀ **Fig. 4** Cuneiform of the *Scelidotherium* Owen, 1839, specimens CORD PZ 4464 and 4586. **a**, proximal view of bone in CORD PZ 4464; **b**, proximal view of bone in CORD PZ 4586; **c**, proximomedial view of bone in CORD PZ 4464;, proximomedial view of bone in CORD PZ 4586; **e**, palmar view of bone in CORD PZ 4464; **f**, palmar view of bone in CORD PZ 4586. *Abbreviations: l*, articular surface for lunar; *m*, medially facing part of proximal surface; *p*, articular surface for pisiform; *r*, ridge probably related to pisiform facet ontogeny; *u*, articular surface for ulna; *un*, articular surface for unciform. Each interpretative drawing is just below the corresponding photograph. On interpretative drawings, grey areas represent articular surfaces; stippled areas represent sedimentary matrix; hatched areas represent breakage. Scale bar equals 10 mm

1/1845:831 (Lund 1842; Winge 1915). Fusion is not clear for CORD PZ 4464. In both CORD PZ 4464 and CORD PZ 4586 the trapezoid is proximodistally flattened (Fig. 5a–e) and approximately triangular in proximal/distal views. Both CORD PZ 4464 and 4586 have a palmar process, which enhances the triangular shape of these bones in proximal view, as in most specimens of *Scelidotherium* (McDonald 1987), and some of *C. chiliense* (McDonald 1987). This contrasts with its absence in most, but not all, specimens of *C. tarijensis* and *C. cuvieri*, and at least one of *V. bucklandi* (Winge 1915; McDonald 1987). In both CORD PZ 4464 and 4586 the trapezoid is dorsopalmarly deeper than mediolaterally wide (ratios are 1.04 and 1.1, respectively; Table 2), unlike scelidotheriine specimens lacking a palmar process (McDonald 1987). They are relatively slightly shallower than in an unspecified *Scelidotherium* specimen in ZMK 1/1845 (ratio: 1.13), but slightly relatively deeper than in *C. cuvieri* (range of ratio: 0.89–0.95), and significantly deeper than in *V. bucklandi* (ratio: 0.73), according to measurements in Winge (1915). In CORD PZ 4586, the dorsal surface of the trapezoid presents an obtuse angle between its medial and distomedial borders (Fig. 5a), as in the scelidotheriine material described by Cuenca Anaya (1995), but in CORD PZ 4464 the borders form an acute angle. In CORD PZ 4586, the trapezoid is quite low at the medial border. The ratio between its maximum height at the medial border and its maximum mediolateral width (0.3; Table 2) more closely approaches the one of *V. bucklandi* (0.44), than that of *C. cuvieri* (range: 0.5–0.61), or *Scelidotherium* (0.76), according to the measurements in Winge (1915). In CORD PZ 4586, the trapezoid presents a large articular surface for the trapezium-metacarpal I medially. That articular surface is dorsopalmarly elongate, and occupies the central part of the medial surface. It is strongly concave dorsopalmarly, but not proximodistally. In CORD PZ 4586, the articular surface for the metacarpal II is convex dorsally and concave palmarly. It presents a clear, prominent, blunt, and oblique edge on its dorsal part, which separates regions of the facet with different orientations (Fig. 5b). This relatively sharp inflection is shared with the Montehermosan (Miocene–Pliocene) specimen PVUNS 198 (Aramayo 1988), and the specimens of *C. cuvieri* described by Winge (1915); it is unlike the even curvature of this articular facet in *V. bucklandi* (Winge 1915).

Magnum In CORD PZ 11293, this bone is clearly free from fusion to the trapezoid (Fig. 5g), as in PVUNS 198 (Aramayo 1988). In CORD PZ 4586 and 11293, the articular surface for the scaphoid is not subdivided (Fig. 5c, g), as in *C. chiliense* (Sefve 1915) and *C. cuvieri*, but not *V. bucklandi* (Winge 1915). In CORD PZ 4586 and 11293, the scaphoid articular facet resembles a sinuous band in shape (Fig. 5c, g), unlike the crescentic shape of the *S. leptocephalum* specimen from Rosario de la Frontera (Esteban et al. 1992). In CORD PZ 4586 and 11293, the dorsal end of the articular surface does not taper, but does in the *S. leptocephalum* specimen from Rosario de la Frontera (Esteban et al. 1992). In CORD PZ 4586, the dorsal portion of the articular surface for the scaphoid is nearly as wide as the palmar one, whereas in CORD PZ 11293 the scaphoid facet narrows dorsally (Fig. 5c, g). In both CORD PZ 4586 and 11293, this facet is mostly dorsopalmarly convex, but its dorsal portion is dorsopalmarly concave. Such a dorsal concave part most closely agrees with the description of *Ps. confusum* by Hirschfeld (1985) than with previous descriptions of the condition as convex in other late Pleistocene scelidotheriines (e.g., *C. chiliense*, *C. cuvieri, S. leptocephalum, V. bucklandi,* Sefve 1915; Winge 1915; Esteban et al. 1992). In both CORD PZ 4586 and 11293, the palmar portion of the scaphoid facet is dorsopalmarly convex, as in the *S. leptocephalum* specimen from Rosario de la Frontera (Esteban et al. 1992), unlike the flat facet of *V. bucklandi* (Winge 1915). In CORD PZ 11293 the ridge between the articular surfaces for scaphoid and lunar is sharper than in CORD PZ 4586. In both CORD PZ 4586 and 11293, the dorsal portion of the articular surface for the lunar is dorsopalmarly concave (Fig. 5h, i), but convex in *V. bucklandi* (Winge 1915). CORD PZ 11293 presents a single articular facet for the trapezoid, which is undivided by edges or non-articular tracts (Fig. 5g). This contrasts with the presence of two distinguishable facets in *V. bucklandi* (Winge 1915) and *C. chiliense* (Sefve 1915). The articular facet for the unciform is dorsopalmarly elongated and proximodistally narrow (Fig. 5h, i). In CORD PZ 11293, the facet is strongly dorsopalmarly concave, except at its dorsal end (Fig. 5j), as in the *S. leptocephalum* specimen from Rosario de La Frontera (Esteban et al. 1992). In CORD PZ 4586, the dorsopalmar concavity is nearly absent (Fig. 5d). In both specimens, the dorsal end of the facet is dorsopalmarly convex. In CORD PZ 11293, the unciform facet does not contact the articular surface for the metacarpal III (Fig. 5i), unlike in *C. chiliense* (Sefve 1915). In both CORD PZ 4586 and 11293, the articular surface for the metacarpal II is well developed on the dorsal portion of the bone distal surface (Fig. 5b, k), as in *C. chiliense* (Sefve 1915), but not *V. bucklandi* (Winge 1915). In CORD PZ 11293, this facet is dorsopalmarly longer than

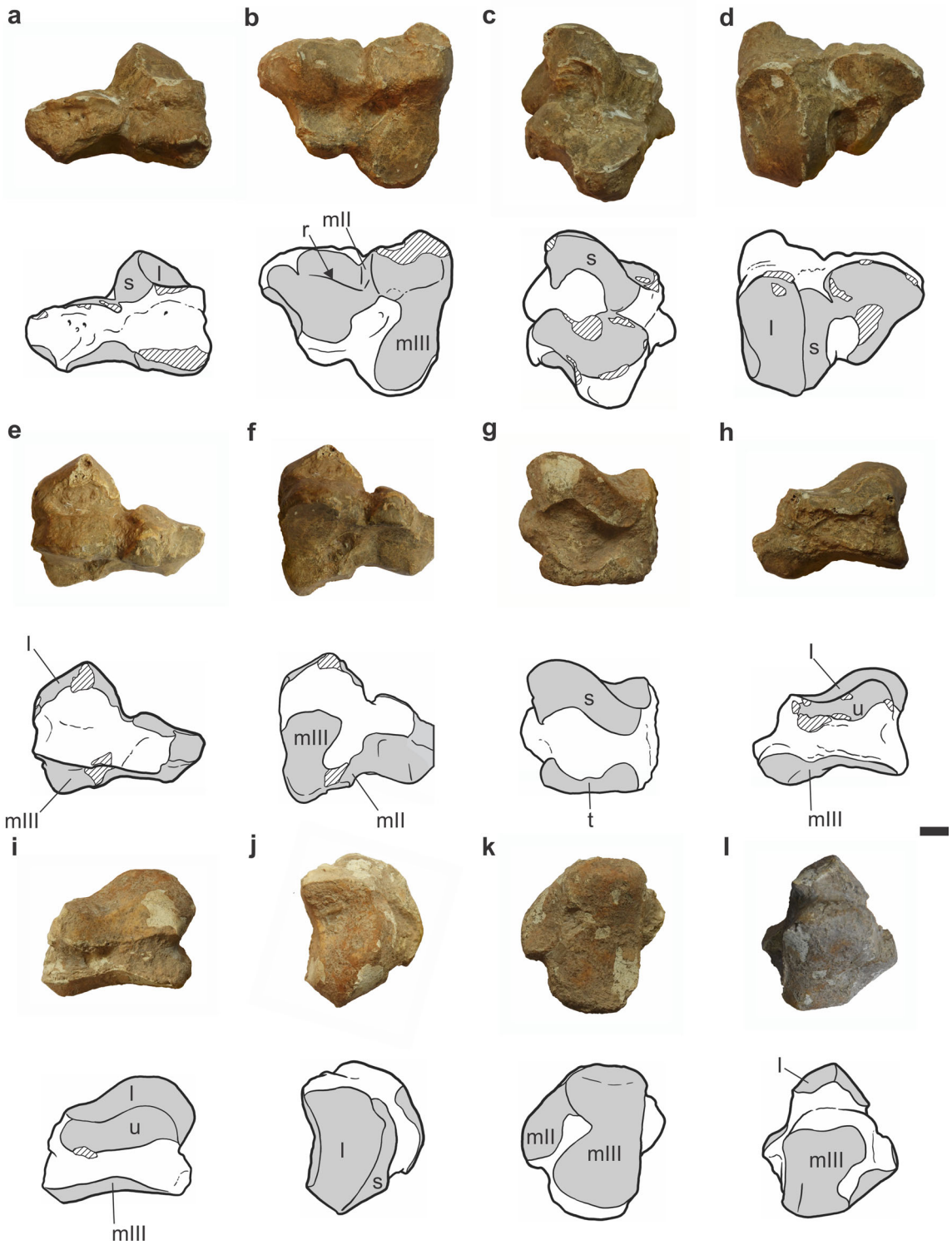

mediolaterally wide, and extends along the dorsal two-thirds of the bone distal aspect (Fig. 5k). This facet is dorsopalmarly convex on its dorsal portion but dorsopalmarly concave at the palmar one. In both CORD PZ 4586 and 11293, the articular surfaces for metacarpals II and III contact dorsally (Fig. 5 k). In both CORD PZ 4586 and 11293, they do not contact at the middle (Fig. 5b, k), as in *C. cuvieri*, but not *V. bucklandi* (Winge 1915). In CORD PZ 4586, there is no contact palmar to that point (Fig. 5b), as in a specimen of *C. cuvieri* (Winge 1915). In both CORD PZ 4586 and 11293, the articular surface for metacarpal III is dorsopalmarly longer than mediolaterally wide (Fig. 5b, k), and reaches the palmar end of the bone. In CORD PZ 4586 and 11293, the articular surface for metacarpal III is not remarkably narrow dorsally (Fig.

◀ **Fig. 5** Trapezoid and magnum of the *Scelidotherium* Owen, 1839, specimens CORD PZ 4586 and 11293. **a**, dorsal view of co-ossified bones in CORD PZ 4586; **b**, distal view of co-ossified bones in CORD PZ 4586; **c**, proximomedial view of co-ossified bones in CORD PZ 4586; **d**, proximal view of co-ossified bones in CORD PZ 4586; **e**, palmar and slightly distal view of co-ossified bones in CORD PZ 4586; **f**, palmodistal view of co-ossified bones in CORD PZ 4586; **g**, proximomedial view of magnum in CORD PZ 11293; **h**, lateral view of magnum in CORD PZ 4586; **i**, lateral view of magnum in CORD PZ 11293; **j**, proximal view of magnum in CORD PZ 11293; **k**, distal view of magnum in CORD PZ 11293; **l**, palmodistal view of magnum in CORD PZ 11293, arrow indicates mediodistal corner of trapezoid dorsal surface. *Abbreviations: l*, articular surface for lunar; *mII*, articular surface for metacarpal II; *mIII*, articular surface for metacarpal III on magnum; *r*, ridge on articular surface for metacarpal II on trapezoid; *s*, articular surface for scaphoid; *t*, articular surface for trapezoid; *u*, articular surface for unciform. Each interpretative drawing is just below the corresponding photograph. On interpretative drawings, grey areas represent articular surfaces; hatched areas represent breakage. Scale bar equals 10 mm

5b, k), unlike in *V. bucklandi* (Winge 1915). The dorsal portion of the metacarpal III articular surface is dorsopalmarly convex, and the palmar one is dorsopalmarly concave. In CObut contrasts with the shortened,RD PZ 4586, this dorsopalmar concavity is much deeper than in CORD PZ 11293 (Fig. 5h, i). In this, therefore, CORD PZ 4586 more closely resembles the *S. leptocephalum* specimen from Rosario de La Frontera (Esteban et al. 1992). In both CORD PZ 4586 and 11293, the palmar portion of the articular surface for the metacarpal III is mediolaterally convex, but more so in the latter (Fig. 5e–l). In CORD PZ 4586, the dorsal portion of the metacarpal III articular surface presents a marked, nearly transversely oriented edge that divides the medial part of the facet into two areas; in CORD PZ 11293 it is fainter (Fig. 5b, k). In CORD PZ 4586, the portion of the metacarpal III articular surface dorsal to this edge is slightly mediolaterally concave, but in CORD PZ 11293 it is slightly mediolaterally convex (Fig. 5f, l).

Unciform The proximal aspect of the bone presents a prominent bump at its mediopalmar region, and forms part of the articular facets for the lunar and cuneiform. These facets are convex at the bump (both mediolaterally and dorsopalmarly). In both CORD PZ 4586 and 11293, the articular surface for the lunar exposes on the proximal aspect (Fig. 6a, b), unlike in the *S. leptocephalum* specimen from Rosario de la Frontera (Esteban et al. 1992). In CORD PZ 4464, 4586, and 11293, the lunar articular facet is dorsopalmarly elongated, reaches the dorsal border of the proximal surface (Fig. 6a, b), and separates the articular facets for the magnum and cuneiform. That dorsal extension is shared with the *S. leptocephalum* specimen from Rosario de la Frontera (Esteban et al. 1992) and *C. cuvieri* (Winge 1915), but contrasts with the shortened, palmarly restricted facet of *V. bucklandi* (Winge 1915). In CORD PZ 4586 and 11293, the facet is roughly a skewed

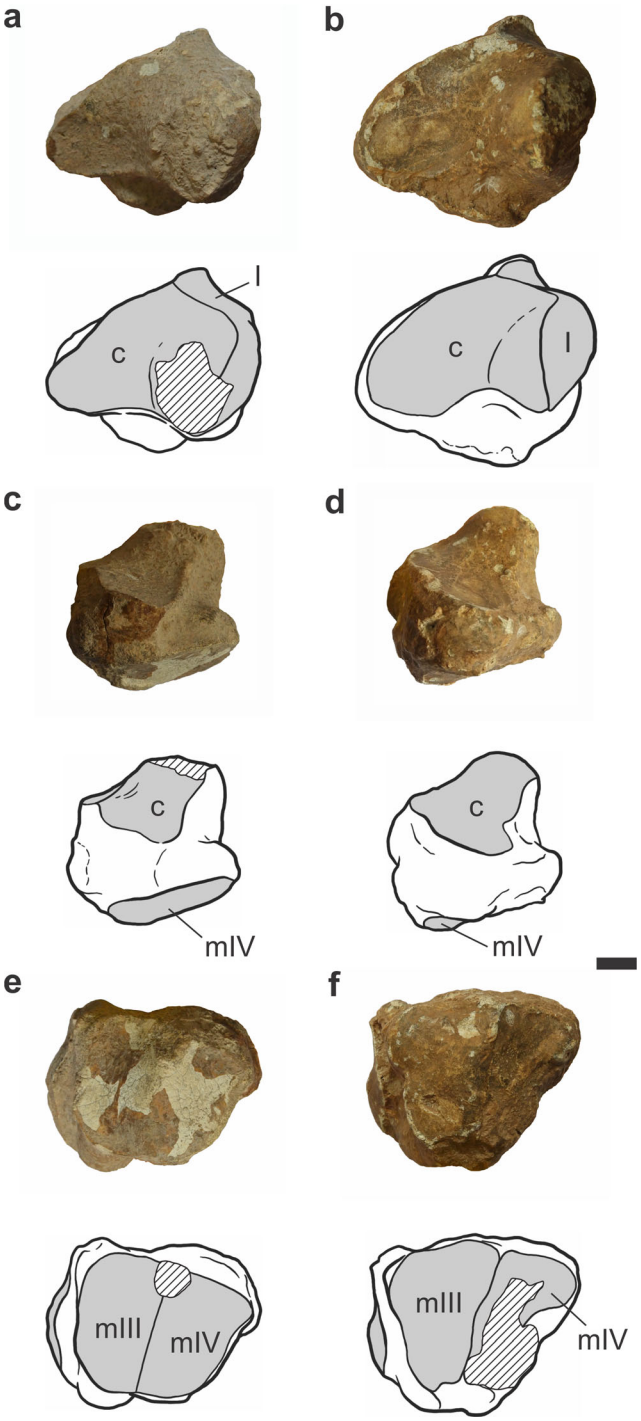

Fig. 6 Unciform of the *Scelidotherium* Owen, 1839, specimens 4586 and 11293. **a**, proximal view of bone in CORD PZ 11293; **b**, proximal view of bone in CORD PZ 4586; **c**, lateral view of bone in CORD PZ 11293; **d**, lateral view of bone in CORD PZ 4586; **e**, distal view of bone in CORD PZ 11293; **f**, distal view of bone in CORD PZ 4586. *Abbreviations: c*, articular surface for cuneiform; *l*, articular surface for lunar; *mIII*, articular surface for metacarpal III; *mIV*, articular surface for metacarpal IV. Each interpretative drawing is just below the corresponding photograph. On interpretative drawings, grey areas represent articular surfaces; hatched areas represent breakage. Scale bar equals 10 mm

parallelogram in shape, unlike the subrectangular shape of the *S. leptocephalum* specimen from Rosario de la Frontera (Esteban et al. 1992). In CORD PZ 4586 and 11293, it does not extend on the medial surface to encroach the articular facet for the magnum, unlike in some specimens of *C. cuvieri* (Winge 1915). In CORD PZ 4586 and 11293, the articular surface for the cuneiform is irregularly reniform in proximal view, unlike the subrectangular shape of the *S. leptocephalum* specimen from Rosario de la Frontera (Esteban et al. 1992). In CORD PZ 4586 and 11293, the surface is approximately saddle-shaped. In CORD PZ 11293, the lateral portion of the cuneiform articular surface is dorsopalmarly slightly concave (Fig. 6c), as in the *S. leptocephalum* specimen from Rosario de la Frontera (Esteban et al. 1992). In CORD PZ 4586, it is less concave (Fig. 6d), and in CORD PZ 4464, it is slightly convex. In CORD PZ 4464, 4586, and 11293, the cuneiform articular surface is dorsopalmarly concave at its mediodorsal region and dorsopalmarly convex at its mediopalmar region, unlike the flat condition of the medial portion of the facet of the *S. leptocephalum* specimen from Rosario de la Frontera (Esteban et al. 1992). In CORD PZ 11293, on the medial aspect, the articular facet for the magnum is dorsopalmarly elongate, and irregular in shape, unlike the subtriangular shape of the *S. leptocephalum* specimen from Rosario de la Frontera (Esteban et al. 1992). In both CORD PZ 4586 and 11293, the metacarpal III articular facet faces mostly distally. In both specimens it is saddle-shaped, dorsopalmarly convex and a mediolaterally concave, unlike the flat or pit-like relief of *C. cuvieri* or the concave relief of *V. bucklandi* (Winge 1915). In both CORD PZ 4586 and 11293, the shape of the articular surface for the metacarpal III is approximately quadrilateral, with rounded medial angles (Fig. 6e, f), instead of subcircular as in the *S. leptocephalum* specimen from Rosario de la Frontera (Esteban et al. 1992). In both CORD PZ 4586 and 11293, the metacarpal IV articular surface faces mostly distally and is roughly saddle-shaped in its dorsal portion, specifically dorsopalmarly convex and mediolaterally concave. In CORD PZ 11293, the middle and palmar portions are convex to flat. The facet is not undulating, unlike in some specimens of *C. cuvieri* (Winge 1915). In CORD PZ 11293, the outline of the articular facet for metacarpal IV is dorsopalmarly elongated, unlike the subcircular shape of the *S. leptocephalum* specimen from Rosario de la Frontera (Esteban et al. 1992). In CORD PZ 4586 and 11293, the articular surface for metacarpal IV presents a distinct dorsal border, continuing the lateral and medial borders at clear angles. In CORD PZ 4464, 4586, and 11293, an articular facet for metacarpal V is lacking, as in most other described specimens of *Scelidotherium* and a single *C. cuvieri* specimen (Winge 1915; McDonald 1987; Esteban et al. 1992). This contrasts with the presence of the facet in *V. bucklandi*, two *Scelidotherium* specimens, and most *C. cuvieri* specimens (Winge 1915; McDonald 1987).

Trapezium-Metacarpal I In CORD PZ 4464 and 4586, the trapezium and metacarpal I are co-ossified and their contact is indicated by a rugose, raised ridge on the palmar surface of the bone. In CORD PZ 4586, the ridge continues on the dorsal surface (Fig. 7a), but in CORD PZ 4464 it does not (Fig. 7b). In both CORD PZ 4464 and 4586, the element is axioabaxially wider proximally. In CORD PZ 4464, abaxially to the articular facet for the trapezoid, the proximal surface of the bone is saddle-shaped (axioabaxially concave and a dorsopalmarly convex) (Fig. 7c). In CORD PZ 4586, the surface is similar, but just concave at its axial portion (Fig. 7d). In CORD PZ 4464, the surface bears a smooth articular facet at

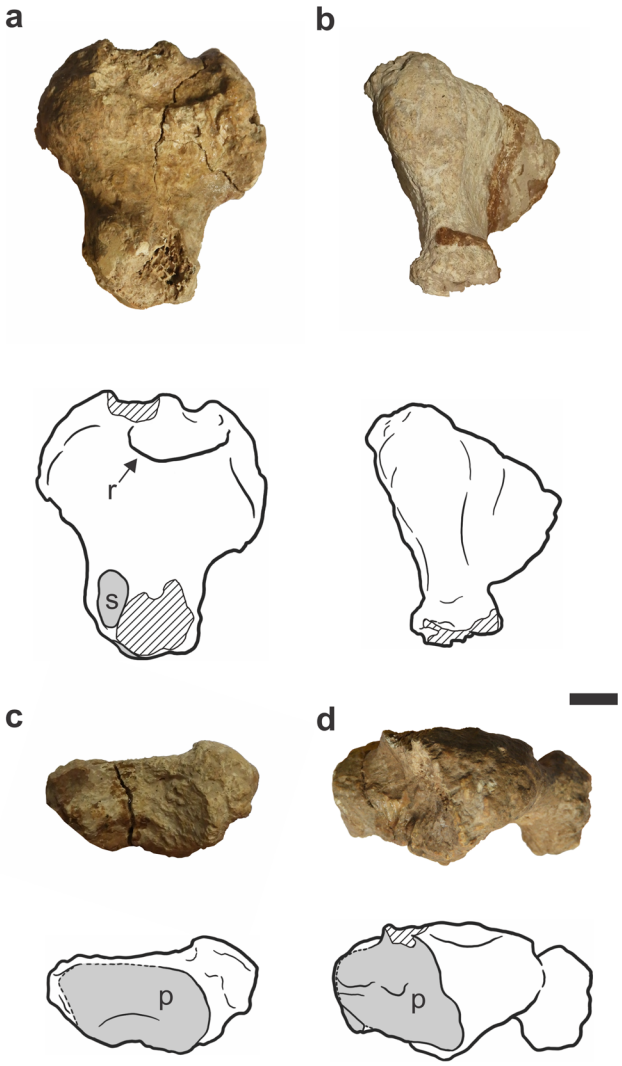

Fig. 7 Co-ossified trapezium-metacarpal I of the *Scelidotherium* Owen, 1839, specimens CORD PZ 4464 and 4586. **a**, dorsal view of bone in CORD PZ 4586; **b**, distodorsoabaxial view of bone in CORD PZ 4464; **c**, proximal view of bone in CORD PZ 4464; **d**, proximoabaxial view of bone in CORD PZ 4586. *Abbreviations: p*, proximal surface; *r*, ridge probably representing suture between trapezium and metacarpal I; *s*, articular surface for possible sesamoid. Each interpretative drawing is just below the corresponding photograph. On interpretative drawings, grey areas represent articular surfaces; hatched areas represent breakage. Scale bar equals 10 mm

its abaxial portion for the scaphoid, and the rest of the surface is rugose and badly preserved (Fig. 7c). In CORD PZ 4586, the aforementioned smooth articular facet is not present, and the rugosity is more strongly marked (Fig. 7d). In CORD PZ 4586, the articular surface for the trapezoid is a little smaller than the articular surface for the metacarpal II. In CORD PZ 4586, the articular surface for the trapezoid is proximal and adjacent to the articular surface for metacarpal II; both facets met at an obtuse angle. In both CORD PZ 4464 and 4586, the axial knob on the proximal end of the bone is prominent, as in *C. cuvieri* but not *V. bucklandi* (Winge 1915). In CORD PZ 4586, distal articular surface does not reach the abaxial side of the distal end, as in most specimens of *Scelidotherium*, but not the genus *Catonyx* (McDonald 1987). In CORD PZ 4586, the distal articular surface presents a keel on its palmar part. In CORD PZ 4586, a conspicuous articular facet is present on the dorsoaxial surface of the distal end (Fig. 7a), but in CORD PZ 4464 a facet is absent in this position (Fig. 7b).

Metacarpals

Only metacarpals II–V are described in this section. Metacarpal I was described above with the carpal bones because it is co-ossified with the trapezium.

Metacarpal II In CORD PZ 4586, the bone is relatively short compared with its axioabaxial width at the proximal end, yielding a ratio of 0.67 (Table 2), which is larger than those previously reported for other scelidotheriines. Among these, it more nearly approaches *C. cuvieri* (range of ratio: 0.56–0.64); then *C. chiliense* (range of ratio: 0.57–0.59); then *Scelidotherium* (range of ratio: 0.56–0.57), and finally *V. bucklandi* (range of ratio: 0.52–0.54), according to published measurements (Sefve 1915; Winge 1915; Pujos 2000). In CORD PZ 4586, the proximal aspect of the bone is approximately triangular and bears the articular surfaces for the trapezoid and magnum. The articular surface for the trapezoid occupied most of the proximal aspect, and reaches both its dorsal and palmar borders. The facet is dorsally concave and palmarly convex. In CORD PZ 4586, the articular facet for the magnum is an axioabaxially narrow band axial and adjacent to the articular surface for the trapezoid. In CORD PZ 4586, it extends into the dorsal part of the proximal surface and thus precludes the facet for the trapezoid to reach the axial border of the proximal surface, unlike in *V. bucklandi* (Winge 1915). In CORD PZ 4586, the articular surface for the magnum is dorsopalmarly excavated as an acute angle, but axioabaxially nearly straight. In CORD PZ 4586, the articular surface for the trapezium-metacarpal I is slightly concave dorsopalmarly, and slightly convex proximodistally. In CORD PZ 4586, the facet is dorsopalmarly elongate, dorsally expanded and palmarly narrow, whereas it is subrectangular in the *S. leptocephalum* specimen from Rosario de La Frontera (Esteban et al. 1992). In CORD PZ 4586, the axial aspect presents a proximodistally extended and dorsopalmarly narrow flange, whose tip points distally (Fig. 8a). This process is adjacent to part of the badly preserved articular surface for metacarpal III. The portion just distal and dorsal to this process is proximodistally straight or slightly convex, and dorsopalmarly concave. In CORD PZ 4586, there is no evidence that a sulcus divided the articular surface for the metacarpal III, unlike in the *S. leptocephalum* specimen from Rosario de La Frontera (Esteban et al. 1992). The distal articular surface is dorsopalmarly elongated. The midline carina on the distal articular surface is thicker dorsally and thinner palmarly (Fig. 8b), as in *C. cuvieri*, but not *V. bucklandi* (Winge 1915). The carina is palmarly sharper. In CORD PZ 4586, the border of the midline carina is nearly straight in axial/abaxial views, unlike the convex profile of several specimens of *V. bucklandi* (Winge 1915). In CORD PZ 4586, the carina is slightly bowed axialwards (Fig. 8b). In CORD PZ 4586, the axial condyle presents a notch at its axial border (Fig. 8b), as in *C. cuvieri*, but not *V. bucklandi* (Winge 1915). In both CORD PZ 4464 and 4586, the proximal part of the axial border of the dorsal surface is distinctively prominent dorsally but does not overlap the abaxial margin of metacarpal III, unlike in some, but not all, *Catonyx* specimens (Winge 1915; McDonald 1987).

Metacarpal III In CORD PZ 4464, the bone narrows dorsopalmarly at midlength. The space separating the articular surfaces for magnum and unciform does not expose on the dorsal surface of the metacarpal when articulated with these two carpals (Fig. 2), as in other scelidotheriine specimens referred to the genera *Scelidotherium* and *Catonyx* (pers. obs.), but unlike *V. bucklandi* (pers. obs.). The axial contours of the bone in dorsal/palmar views are nearly parallel to the long axis of the bone, suggesting an axially facing facet for metacarpal IV. A notch is present on the abaxial border of the distal articular surface.

Metacarpal IV In both CORD PZ 4464 and 4586, the proximal and distal ends are dorsopalmarly deeper than the shaft (Fig. 8c). The proximally facing articular surface for the unciform is dorsopalmarly sinuous: concave at its dorsal part and slightly convex at its palmar part. In CORD PZ 4586, the articular facets for metacarpal III and unciform form an obtuse angle, as in *Scelidotherium* but not *Catonyx* (McDonald 1987). In CORD PZ 4586, the articular facet for the metacarpal V is not in contact with the facet for the unciform, unlike in *Pr. gracillimus*, *V. bucklandi*, and most, but not all, *C. cuvieri* specimens (Winge 1915; Ortega 1967). In CORD PZ 4586, the articular facet for metacarpal III is dorsopalmarly sinuous, slightly concave dorsally and slightly convex palmarly, and proximodistally slightly convex dorsally, but roughly straight

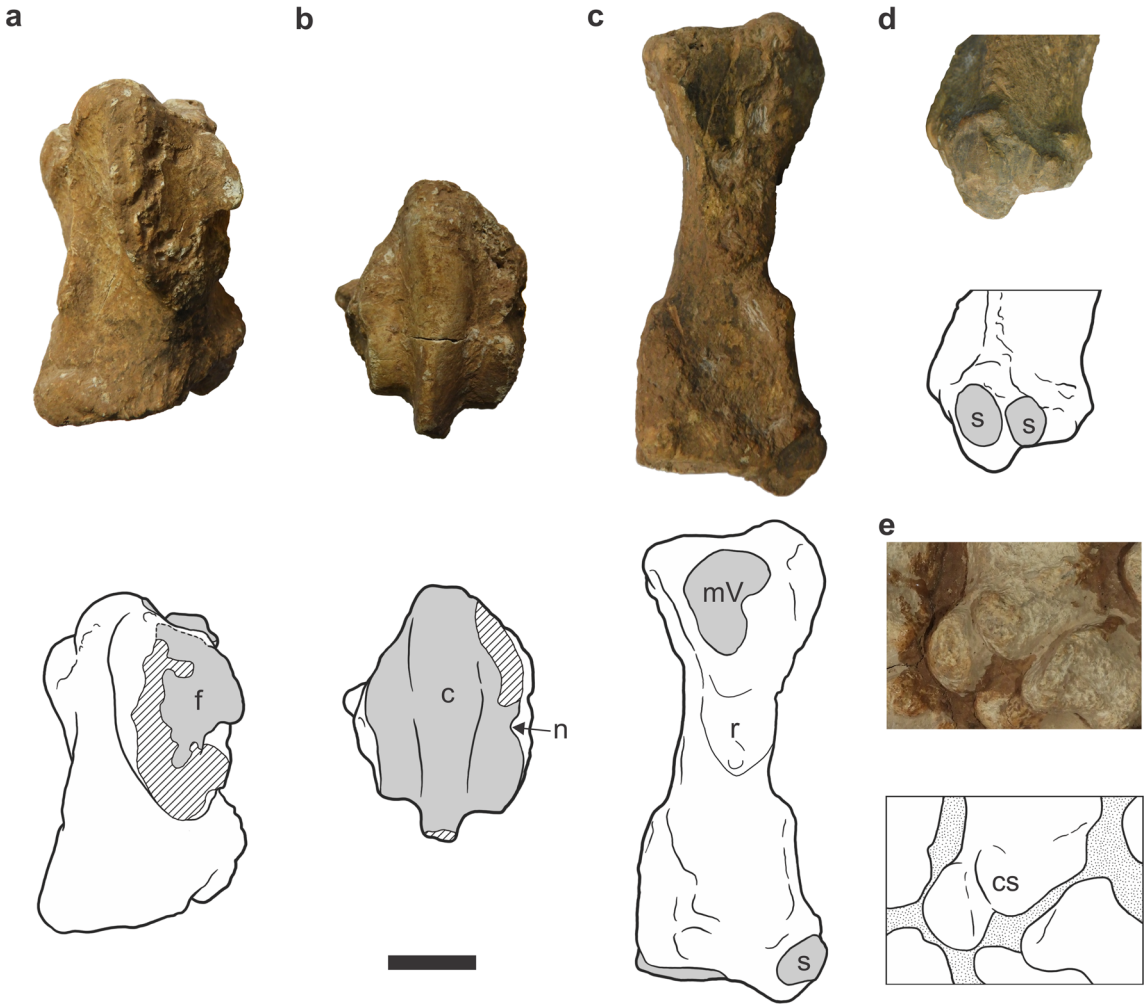

Fig. 8 Metacarpals II and IV of the *Scelidotherium* Owen, 1839, specimens CORD PZ 4464 and 4586. **a**, dorsoaxial view of metacarpal II in CORD PZ 4586; **b**, distal view of metacarpal II in CORD PZ 4586; **c**, proximoabaxial view of metacarpal IV in CORD PZ 4586; **d**, palmar view of distal end of metacarpal IV in CORD PZ 4586; **e**, palmar view of metacarpal IV in CORD PZ 4464. *Abbreviations: c*, carina; *cs*, bulge probably representing co-ossified sesamoid; *f*, projecting flange on axial surface of bone; *mV*, articular surface for metacarpal V; *n*, notch in the border of the axial condyle of the distal end; *r*, rugose area; *s*, articular surface for sesamoid. Each interpretative drawing is just below the corresponding photograph. On interpretative drawings, grey areas represent articular surfaces; stippled areas represent sedimentary matrix; hatched areas represent breakage. Scale bar equals 20 mm

palmarly, unlike the simply concave facet of *V. bucklandi* (Winge 1915). In CORD PZ 4586, on the proximal end of the abaxial surface, the articular surface for metacarpal V is dorsopalmarly concave and proximodistally sinuous, proximally convex and distally concave. In both CORD PZ 4464 and 4586, the shaft is axioabaxially wider than dorsopalmarly deep, as in other *Scelidotherium* specimens (McDonald 1987). In CORD PZ 4586, the distal articular keel is clearly marked and relatively less expanded dorsopalmarly than in *Pr. gracillimus* (Ortega 1967). Only the axial condyle is present on the distal articular surface, and the border of the keel midline protrudes axiodistally. In CORD PZ 4586, two articular facets for the sesamoid bones are present palmar to the distal articular surface (Fig. 8d). In CORD PZ 4464, articular facets for sesamoids are not visible, but a bulge is present in the place corresponding to the axial sesamoid (Fig. 8e).

Metacarpal V In CORD PZ 4464, the proximal surface does not have an articular surface for the unciform, as has been previously described in other individuals of the genus (Schulthess 1920; McDonald 1987). The palmar surface presents three prominent oblique crests.

Phalanges

Proximal Phalanx of Digit I In both specimens CORD PZ 4464 and 4586, this phalanx is present, unlike in some *Scelidotherium* specimens (Burmeister 1881). In CORD PZ 4464 and 4568, the phalanx presents a sulcus on its proximal surface for the carina of the trapezium-metacarpal I. The sulcus in the latter specimen is very extensive dorsopalmarly, reaching the dorsal half of the facet. In both specimens, on the palmar aspect, the sulcus corresponds to an indentation of

the proximal border, unlike in most described specimens of *C. cuvieri* (Winge 1915). In both CORD PZ 4464 and 4586, the distal end is badly preserved, and the presence or absence of a distal articular facet cannot be determined. In CORD PZ 4586, the palmar part of the distal end presents a raised surface that has a low sagittally oriented ridge in the middle. In both CORD PZ 4464 and CORD PZ 4586, the bone lacks any evidence of being the result of fusion of two originally distinct phalanges.

Proximal Phalanx of Digit II This phalanx, recovered only in CORD PZ 4464, is proximodistally flattened, and in dorsal view presents a centered notch that marks the dorsal limit of the groove for the articular carina of the metacarpal.

Intermediate Phalanx of Digit II This phalanx, recovered only in CORD PZ 4464, presents a width among the distal articular condyles that is slightly lesser than that of the proximal end.

Distal Phalanx of Digit II In both CORD PZ 4464 and 4586, the phalanx is about as large as the distal phalanx of the digit III of the manus, unlike the relatively smaller phalanx in *C. cuvieri* and *V. bucklandi* (Winge 1915). In CORD PZ 4586, the proximal articular surface presents two concave surfaces for the distal condyles of the intermediate phalanx separated by a wide sagittal ridge. In CORD PZ 4586, the ungual process is dorsopalmarly depressed (Fig. 9a, b), as in *C. cuvieri*, but unlike the axioabaxially compressed phalanx of *V. bucklandi* (Winge 1915). Prominent acute longitudinal edges are present on the axial and abaxial sides of the ungual process. In CORD PZ 4586, the process presents an axial side flatter than the abaxial, as in *C. cuvieri,* but unlike the more symmetrical flattening of the sides in *V. bucklandi* (Winge 1915).

Proximal Phalanx of Digit III In both CORD PZ 4464 and 4586, this bone is preserved articulated to phalanx III-2, with sediment interposed in the peripheral parts of their contact. In CORD PZ 4586, the abaxial palmar process of phalanx III-1 is preserved relatively closer to that of phalanx III-2 than in CORD PZ 4464. In both specimens, as much as exposed, phalanx III-1 is proximodistally shorter than axioabaxially wide or dorsopalmarly deep. In CORD PZ 4586, the groove on the proximal articular surface for the distal carina of the metacarpal clearly narrows palmarwards, unlike in *V. bucklandi* (Winge 1915). Axially to the sulcus for the carina on the proximal articular surface, the articulation is narrow, reduced, and closer to the palmar border than to the dorsal, as in *C. cuvieri*, but unlike the sizable facet of *V. bucklandi* (Winge 1915).

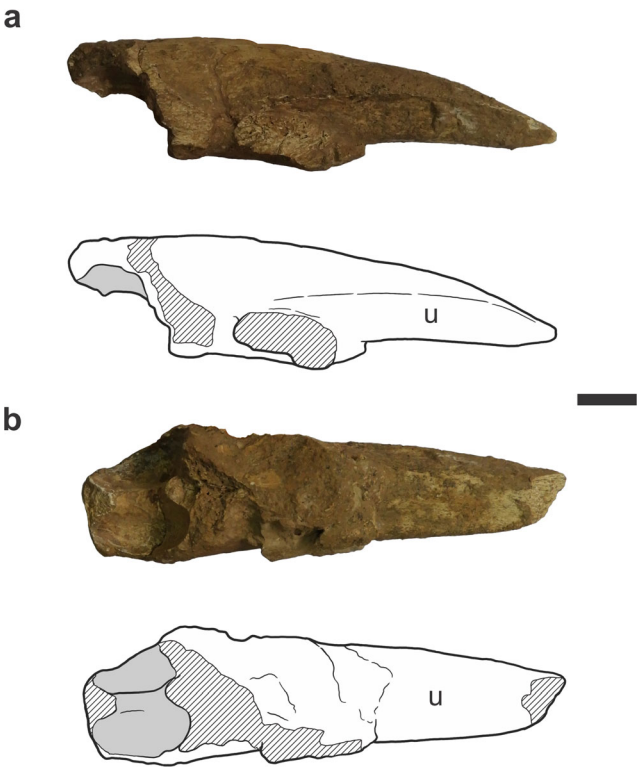

Fig. 9 Distal phalanx of digit II of the manus of the *Scelidotherium* Owen, 1839, specimen CORD PZ 4586. **a**, abaxial view; **b**, palmar view. *Abbreviations: u*, ungual process. Each interpretative drawing is just below the corresponding photograph. On interpretative drawings, grey areas represent articular surfaces; hatched areas represent breakage. Scale bar equals 20 mm

In CORD PZ 4464 and CORD PZ 4586, an articular surface for a sesamoid is not clear, unlike the clear facet present in *V. bucklandi* (Winge 1915).

Intermediate Phalanx of Digit III In both CORD PZ 4464 and CORD PZ 4586, the distal articular surface is a trochlea. In both CORD PZ 4464 and CORD PZ 4586, the distal articular surface faces partially axially (more so in the former), as in *C. cuvieri*, but not *V. bucklandi* (Winge 1915).

Distal Phalanx of Digit III In both CORD PZ 4464 and 4586, the proximal end narrows less in dorsal view than in the distal phalanx of digit II. The distal end of the phalanx is clearly pointed in CORD PZ 4586, contrasting with the rectangular condition of the distal end in other scelidotheriines (McDonald 1987).

Proximal Phalanx of Digit IV In CORD PZ 4464, this phalanx presents a deep depression on its palmar surface. The region of the distal articular surface near the palmoaxial corner is approximately flat. In palmar view, the distal end is more axially set than the proximal.

Intermediate(?) Phalanx of Digit IV In CORD PZ 4464, the most distal preserved element of digit IV presents on the dorsal surface a prominence (Fig. 2). The distal end of the phalanx is unpreserved. In palmar view, the phalanx presents its distal end more axially positioned than the proximal.

Proximal Phalanx of Digit V The distal articular surface faces distoaxially, and the abaxial surface of the bone is very convex proximodistally.

Intermediate(?) Phalanx of Digit V In CORD PZ 4464, this phalanx is free from the proximal phalanx of the fifth digit, as in some, but not all, specimens of *Scelidotherium* (Winge 1915; Cuenca Anaya 1995). It is the shortest and smallest preserved phalanx in CORD PZ 4464. The phalanx narrows distally, but its shape is incompletely exposed.

Other Manual Bones

Palmar Sesamoid (Falciform) In CORD PZ 4464, this dorsopalmarly flattened bone is nearly rectangular, as in *C. cuvieri*, but unlike the rounded bone of *V. bucklandi* (Winge 1915).

Abaxial Sesamoid of Digit II As far as we know, no published work has described this element in other scelidotheriine specimens. In CORD PZ 4464, this bone is characterized by a very prominent palmar keel that turns to extend into the proximal surface.

Abaxial Sesamoid of Digit III As far as we know, no published work has described this element in other scelidotheriine specimens. In CORD PZ 4464, this bone is stouter than in mylodontines such as *Paramylodon harlani* (Owen, 1839) and *M. darwinii* (Stock 1925; Haro et al. 2016), as measured with its axioabaxial width vs. proximodistal length ratio (0.77). The sesamoid presents a prominent oblique ridge on its abaxial side that contrasts with the lesser and more longitudinal structure of *M. darwinii*. The ridge on the abaxial side of the palmar surface is relatively more proximodistally extended than in *M. darwinii*. The articular surface for the abaxial condyle is mediolaterally more concave than in *M. darwinii*. The bone is irregularly pentagonal in cross-section, instead of square as in *M. darwinii* (Haro et al. 2016). The bone is deeper than wide, unlike the depressed element of *Paramylodon harlani* (Stock 1925).

Axial Sesamoid of Digit III As far as we know, no published work described this element in other scelidotheriine specimens. It is quite incomplete, and the preserved parts do not allow confirming there are differences from the condition described for *Paramylodon harlani* by Stock (1925).

Abaxial Sesamoid of Digit IV As far as we know, no published work described this element in other scelidotheriine specimens. This incomplete sesamoid bears a concave articular surface for metacarpal IV and a convex palmar surface. The preserved parts do not allow confirming there are differences from the condition described for *Paramylodon harlani* by Stock (1925).

Phylogenetic Analysis

The phylogenetic analysis of the entire data matrix including *S. leptocephalum*, *S. parodii*, and the specimens PVUNS 198, CORD PZ 4464, 4586, and 11293 as different terminals (Analysis 1) produced 15 MPTs (L: 340.454; CI: 0.624; RI: 0.598), provided in Supplementary Data 1. The strict consensus (Fig. 10a) recovered all the specimens here reported, together with *S. leptocephalum* and *S. parodii*, within a group. Another recovered clade is a trichotomy between *C. cuvieri*, *C. tarijensis*, and *C. chiliense*. *Sibyllotherium guenguelianum* is recovered as the most basal taxon among the Scelidotheriinae. *Neonematherium flabellatum* Ameghino, 1904, is recovered as most closely related to the remaining scelidotheriines than *Sibyllotherium guenguelianum*. These remaining scelidotheriines form a large polytomy in which the only recognized groups are those corresponding to the genera *Scelidotherium* and *Catonyx*. Included outgroups to the Scelidotheriinae present the same topology as in Gaudin (2004). The apparent lack of resolution vanishes when hiding in the consensus the position of the species *Pr. rothi* and *Proscelidodon patrius* (Ameghino, 1888) (Fig. 10b), which are wildcard taxa. Hiding *Pr. rothi* alone exposes a monophyletic clade exclusively formed by the genera *Catonyx* and *Scelidotherium*, here informally called 'clade A'. Hiding the position of *Pr. patrius* alone reveals a clade including *V. bucklandi*, the specimen PVUNS 198, *Pr. rothi*, and the genera *Catonyx* and *Scelidotherium*, which is here informally called 'clade B'. Hiding both *Pr. patrius* and *Pr. rothi*, another clade that includes clade A and the specimen PVUNS 198 emerges, in addition to the formerly mentioned clades. *Proscelidodon rothi* is alternatively recovered as the sister taxon to the genus *Catonyx* or to *V. bucklandi*. *Proscelidodon patrius* is recovered either as: a) part of a trichotomy with the specimen PVUNS 198 and the clade A; b) part of a trichotomy with *Pr. gracillimus* and the clade B; or c) as the sister taxon of *Pr. gracillimus*. The unambiguous apomorphies of all the groups reported in this analysis and the others are provided in Supplementary Data S5. Bremer support and Jackknife frequency values are generally low. When the scores for the included specimens, together with those of *S. parodii* and *S. leptocephalum*, are used to form a single terminal corresponding to the genus *Scelidotherium*, considering all of these form

Fig. 10 Phylogenetic relationships of the Scelidotheriinae, incorporating *Scelidotherium* Owen, 1839, specimens CORD PZ 4464, 4586, and 11293. **a**, Strict consensus of analysis including all terminals and all characters (Analysis 1 in text); **b**, part of reduced strict consensus of Analysis 1, obtained hiding the position of wildcard taxa *Proscelidodon rothi* and *Proscelidodon patrius*; **c** as in a, but merging *Scelidotherium leptocephalum*, *Scelidotherium parodii*, and CORD PZ 4464, 4586, and 11293 into a single terminal, *Scelidotherium* (Analysis 2 in text); **d**, part of reduced strict consensus of Analysis 2, obtained hiding the position of wildcard taxa *Pr. rothi* and *Pr. patrius*; **e**, as in c, but excluding all the characters belonging to the manus (Analysis 3 in text); **f**, as in **c**, but only including the characters belonging to the manus (Analysis 4 in text). Above branches are the respective Bremer support values; below the branches are the Jackknife frequencies

a monophyletic group in the previous analysis, three MPTs (L: 333.925; CI: 0.658; RI: 0.594) are recovered from the analysis (here referred to as Analysis 2). The MPTs are provided in Supplementary Data 2. The strict consensus presents exactly the same groups as in Analysis 1 (Fig. 10c). The reduced strict consensus, after hiding the position of *Pr. patrius* and *Pr. rothi*, is also the same as in Analysis 1 (Fig. 10d). Jackknife frequency and Bremer support values increase compared to Analysis 1, but are still generally low.

The analysis of the data matrix excluding the characters from the manus (here referred to as Analysis 3) produced a single MPT (L: 253; CI: 0.617; RI: 0.601). This tree is provided in Supplementary Data 3. The tree (Fig. 10e) presents the relationships of the basal part, including the scelidotheriine outgroups, *Sibyllotherium guenguelianum* and *N. flabellatum*, identical to the strict consensus of Analysis 2. On the other hand, except in the recovery of the clade represented by a trichotomy between *C. chiliense*, *C. cuvieri*, and *C. tarijensis*, it largely disagrees from the strict consensus of the other analyses regarding the relationships of post-Friasian scelidotheriines. A clade formed by *Pr. rothi* and *V. bucklandi* is recovered in this analysis as the sister taxon to the *Catonyx* group. The clade formed by *Pr. rothi*, *V. bucklandi*, and the species of the genus *Catonyx* presents *Pr. patrius*, *Pr. gracillimus*, and the genus *Scelidotherium* as successive outgroups. Jackknife frequency and Bremer support values are generally larger than in the previous analyses, although they are relatively low for the clades that include species of the genus *Proscelidodon*. The analysis of the data matrix only including the characters from the manus (here referred to as Analysis 4) recovers eight MPTs (L: 75.516; CI: 0.844; RI: 0.694), provided in Supplementary Data 4. The strict consensus (Fig. 10f) recovers a clade formed by *Scelidotherium* and the species of the genus *Catonyx*, and another formed by that clade and the specimen PVUNS 198. Hiding *Pr. patrius* and *Pr. gracillimus* from the strict consensus exposes a clade including *M. darwinii*, *Ps. confusum*, *V. bucklandi*, and the clade formed by *Scelidotherium*, the *Catonyx* species, and

the specimen PVUNS 198. Hiding *Pr. gracillimus*, *V. bucklandi*, and *M. darwinii* from the strict consensus exposes *Pr. patrius* as basal to clade including *Ps. confusum* and the clade formed by *Scelidotherium*, the *Catonyx* species, and the specimen PVUNS 198. Bremer supports and Jackknife frequencies are rather low.

Discussion

Comparative Remarks

The previous comparisons clearly indicate that specimens CORD PZ 4464, 4586, and 11293 more closely resemble other specimens of *Scelidotherium* and *C. cuvieri* than *V. bucklandi*. At least the specimens CORD PZ 4464 and 11293 most closely resemble *Scelidotherium* than *Catonyx*. CORD PZ 4464 more closely resembles other specimens of *Scelidotherium* than *Catonyx* in the relatively deep scaphoid. CORD PZ 11293 shares with *Scelidotherium*, but not *C. chiliense*, an undivided trapezoid articular surface on the magnum. The specimen CORD PZ 4586, on the other hand, most closely resembles *Scelidotherium* in some traits, but *Catonyx* in others. CORD PZ 4586 more closely resembles other specimens of *Scelidotherium* than *Catonyx* in the radial and trapezoid articular facets separated by a considerable interval in the scaphoid, the facets for metacarpal III and unciform on metacarpal IV meeting at an obtuse angle, and the restricted distal articular surface on trapezoid-metacarpal I. On the other hand, the specimen CORD PZ 4586 more closely approaches the range of variation documented in *Catonyx* than that of previously described specimens of *Scelidotherium* in several proportions. Such proportions include the proximodistal height/ulnar facet width in the cuneiform, height of medial part/width in trapezoid, and proximal width/length in metacarpal II. These similarities may relate to the greater number of measurements provided for *C. cuvieri* than for *Scelidotherium* in the comparative work by Winge (1915), which increase the range of variation in the former. In addition, CORD PZ 4586 more closely resembles a specimen of *C. cuvieri* than any one described for *Scelidotherium* in the fusion between magnum and trapezoid. Finally, the three specimens here described share an unciform lacking the articular facet for metacarpal V with most known specimens of *Scelidotherium*, but not most known specimens of *Catonyx*.

Interestingly, many features of the *Scelidotherium* specimens here described differ from those in the *S. leptocephalum* specimen from Rosario de La Frontera reported by Esteban et al. (1992). As previously noted, CORD PZ 4464, 4586, and 11293 all differ from the Rosario de la Frontera specimen in having an unciform with the cuneiform articular facet presenting a dorsopalmarly directed concavity in its mediodorsal region rather than a flat condition. CORD PZ 4586 and 11293 most closely resemble each other than the Rosario de la Frontera specimen, because of having the articular surface for the scaphoid on the magnum band-shaped and sinuous instead of crescentic, with the dorsal part not tapering; and the unciform with the lunar articular surface exposed on the proximal aspect, the cuneiform articular facet irregularly reniform instead of rectangular, the articular surface for metacarpal III quadrangular instead of subcircular, and a non-rectangular parallelogram-shape. CORD PZ 4464 and 4586 share the articular surface for the ulna on the cuneiform roughly triangular, rather than subcircular as in the Rosario de la Frontera specimen. These differences may imply that the specimens here described are taxonomically distinct from the Rosario de la Frontera specimen, and would therefore do not belong to the species *S. leptocephalum*. Indeed, there is no evidence supporting the referral of CORD PZ 4464, 4586, and 11293 to that species, even if their Pleistocene age is suggestive—such evidence will only emerge in the form of overlapping material of *S. parodii* and/or further study on the variation in overlapping material of *S. leptocephalum*. Alternatively, the species *S. leptocephalum* would present a high variability in hand structure. That the latter is the case is consistent with the variability in manual structure described for *C. cuvieri* and *V. bucklandi* by Winge (1915), and in species of the genera *Catonyx* and *Scelidotherium* by McDonald (1987). The phenotypic variation found between the specimens here reported and the Rosario de La Frontera one may indicate the later belongs to a different geographical subspecies, which is possible considering all the specimens here described come from localities in the Córdoba Province that are at least 590 km from Rosario de la Frontera.

Although the presence of geographical variation has been considered in the cases of differences between specimens assigned to the same species that come from different regions, in the case of *C. chiliense* by McDonald (1987) and in the case of *C. cuvieri* by Corona et al. (2013), these studies did not go beyond proposing the possibility. The possible reason is that larger samples are required to find statistically significative differences between populations; at least this holds true for the present case. A larger wealth of material of *Scelidotherium* coming from Rosario de la Frontera, the Córdoba Province, and anywhere in between, is required to test the hypothesis of geographical variation in *Scelidotherium*.

Phylogenetic Considerations

The position of the specimens CORD PZ 4464, 4586, and 11293, closer to the species in the genus *Scelidotherium* than to those in the genus *Catonyx* in Analysis 1, is compatible with referring these specimens to the genus *Scelidotherium* (as in Haro et al. 2016; Krapovickas et al. 2017), and not with referral to *Catonyx* or any other previously recognized genus,

on the grounds of parsimony. Their position is also compatible with the possibility that these specimens represent new genera, but we consider it more conservative to refer them to *Scelidotherium* given that the manus is unknown in one of the two species of the genus. The inclusion of new manual characters in Analysis 2 that supports a phylogenetic scheme in which *Scelidotherium* and *Catonyx* are more closely related to each other than either is to with *V. bucklandi* contradicts the results of Cartelle et al. (2009), Miño-Boilini (2012), and Miño-Boilini et al. (2014), but matches the pre-cladistic taxonomic scheme of Winge (1915), as well as the phylogenetic ideas of Kraglievich (1923), mostly based on upper tooth shape. When all the parsimony-informative characters, except for those belonging to the skeleton of the hand, are included, the interrelationships between the genera *Scelidotherium*, *Catonyx*, and *Valgipes* inferred by Cartelle et al. (2009) are supported. The analysis of hand characters alone supported the close relationship between *Scelidotherium* and *Catonyx*, and the basal position of *Valgipes*, as in the complete dataset, and unlike the other incomplete dataset. However, unlike all the other analyses, it recovered *Ps. confusum* closer to the genera *Scelidotherium* and *Catonyx* than *Pr. patrius*. Thus, both partial analyses do share only some of the groups recovered in the complete analysis, and contradict it regarding some groups. It is apparent both partial datasets contribute resolution for different groups in the complete analysis, and the result of their inclusion is not superfluous.

The results of the complete analyses allowed supporting the assignment of the genera *Valgipes*, *Neonematherium* Ameghino, 1904, *Sibyllotherium* Scillato-Yané and Carlini, 1998, and *Proscelidodon*, but not *Nematherium*, to the Scelidotheriinae, by using *H. longiceps*, *Choloepus*, and the mylodontines *M. darwinii* and *Ps. confusum* as additional outgroups. Our results indicate the use of the added outgroups, in which the osteology of the manus is better known than in the genus *Nematherium*, has been of fundamental importance in recognizing the derived nature of the similarities shared by the genera *Scelidotherium* and *Catonyx* but not *V. bucklandi*. With regard to the position of *N. flabellatum*, our analyses 1 and 3 support the results of Miño-Boilini (2012, 2014) regarding its basal position, which is compatible with its comparatively early geological age, over the hypothesis of close relationships to *Scelidotherium* supported by McDonald and Perea (2002) and Cartelle et al. (2009). The non-monophyletic relationships of the species of the genus *Proscelidodon* are supported in all the present and aforementioned previously published works. The scarcity of material from the skeleton of the manus in the species of that polyphyletic genus is probably responsible for their ambiguous position in our analysis, in face of the change in position of the scelidotheriines for which the hand characters are better known.

The present results allowed testing the alternative generic assignments of the specimen PVUNS 198, either to the genus *Proscelidodon*, as proposed by Aramayo (1988), or to the genus *Scelidotherium*, as proposed by Esteban et al. (1992), on the basis of the lack of articulation between unciform and metacarpal V. The latter hypothesis presents the problem that on the same ground the specimen can be referred to *C. cuvieri*. The position of that specimen basal to the dichotomy between the genera *Scelidotherium* and *Catonyx* in Analyses 1, 2, and 4 (the specimen is not included in analysis 3) indicates rejection of the Esteban et al.'s (1992) assignment. The assignment to *Proscelidodon* cannot be rejected or supported, however, given the variable position of the two species of the genus, *Pr. patrius* and *Pr. rothi*. In no MPT produced by the Analyses 1, 2, or 4 is the specimen PVUNS 198 recovered as more closely related to some species of the genus than to other scelidotheriine taxa. However, lack of resolution at the trichotomy between the specimen PVUNS 198, *Pr. patrius*, and the clade A admits as a possible resolution the grouping of the former two terminals, so the reference to that genus and species is not rejected nor supported. It is thus possible that some specimens of *Pr. patrius* lacked the facet, as in *S. leptocephalum* and *C. cuvieri*. Considering there are specimens with the facet in the genera *Scelidotherium* and *Catonyx* (Winge 1915; McDonald 1987), and others without it in the latter two genera, the possibility of variation in this regard on the genus *Proscelidodon* would imply that the feature is variable in the three main genera of the Scelidotheriinae, and thus of minor importance for systematics. On stratigraphic grounds, the possibility that PVUNS 198 belongs to *Pr. patrius*, which is the only scelidotheriine, and quite abundant, in the same beds (Ameghino 1888; Taglioretti et al. 2014), seems high. A thorough comparative study on the osteology of the manus of the reported Montehermosan scelidotheriine material, for which published data are scarce and insufficient, will be required to address this point. Our results indicate the *Scelidotherium-Catonyx* divergence seems to be at least Chapadmalalan in age according to our results, considering the age of the oldest unequivocal member of these clades, namely *S. parodii*, and the oldest known possible member, namely *Pr. rothi*. The *Scelidotherium-Valgipes* divergence would be at least Montehermosan in age, given the age of the oldest unequivocal member of these clades, namely specimen PVUNS 198. Our data indicate the *Scelidotherium-Catonyx* divergence would not have been posterior to the Chapadmalalan, given the age of the oldest unequivocal member of these clades, *S. parodii*.

Our results clearly differ from previous scelidotheriine phylogenies, which presented fewer characters from the skeleton of the manus, in the position of the genus *Scelidotherium* and the more resolved position of *Pr. gracillimus*. Other phylogenetic studies incorporating postcranial characters into data matrices dominated by cranial, mandibular, and dental

characters also change the relationships inferred by the cranial, mandibular, and dental characters alone. For example, the analysis of Haro et al. (2017), which incorporated postcranial characters to the large data matrix of Gaudin (2004), contradicted the results of the latter in the position of the genera *Lestodon* Gervais, 1855, and *Thinobadistes* Hay, 1919. The analysis of Boscaini et al. (2019) contradicted the results of Gaudin (2004) in the position of *Paramylodon harlani* and *M. darwinii*, in addition to that of *Lestodon* and *Thinobadistes*. The analysis of Amson et al. (2017) on megatherian sloths contradicted the results of Gaudin (2004) regarding the position of basal megatherian genera. All of this indicates that the incorporation of further postcranial data into data matrices allows testing hypotheses based on cranial, mandibular, and dental data and surveying the postcranium for characters that vary between taxa is therefore a worthy enterprise. As in previous phylogenetic analyses based on morphology, such as Gaudin (2004), our analysis fails to recover *Choloepus* as a mylodontine, contrasting with recent paleoproteomic results (Presslee et al. 2019). Despite this, and the very different aspect of the hand of *Choloepus* compared with that of mylodontines (Owen 1842), our comparisons include a similarity between this genus and mylodontines more derived than *Ps. confusum*, namely the dorsopalmarly convex dorsal part of the articular surface for the scaphoid on the magnum (CORD PZ 4570; DMNS 6458; pers. obs.). *Choloepus* also resembles mylodontids more than other sloths in the lack of the ungual phalanx of digit IV (Schulthess 1920). Finally, and surprisingly, many features of the manus of *Choloepus* resemble those of scelidotheriines close to *Scelidotherium*. These include the lack of concavity in the articular surface for the ulna on the cuneiform, at least half of the articular facet for metacarpal II positioned in the dorsal part of the magnum, the absence of an articular facet for the metacarpal V on the unciform (through by metacarpal loss in *Choloepus*; Schulthess 1920), and the presence of a notch on the axial border of the distal articular surface of metacarpal II. Further comparative study of the manus of *Choloepus* seems therefore promising to provide useful tests to currently contradicting phylogenetic hypotheses based mostly on the head skeleton or molecules.

Anatomical Interpretations

Two strange features in the lunar of unspecified '*Scelidotherium*' materials were described by Ortega (1967): (1) facet for the magnum wider palmarly than dorsally (unlike CORD PZ 4586 and other scelidotheriine material); and (2) ridge on that facet closer to the palmar border than to the dorsal (also unlike CORD PZ 4586 and *C. cuvieri*). The condition of that material would be the same as that of other scelidotheriines if the orientation of the lunar in the unspecified '*Scelidotherium*' materials was misinterpreted by Ortega (1967), confusing dorsal for palmar. Fewer assumptions are required if Ortega (1967) misoriented the bone, than by inferring two autapomorphies in the unspecified '*Scelidotherium*' materials he examined. On the cuneiform, the similarity in contour of the pisiform articular facet in CORD PZ 4464 and the facet plus adjacent curved ridge in CORD PZ 4586 suggests the ridge corresponds to the border of the articular facet in some moment of the ontogeny (either previous or later to the preserved stage).

Regarding the trapezium-metacarpal I, the rugose, raised ridge on the palmar surface of the specimens CORD PZ 4464 and 4586, and on the dorsal surface of the former, likely represents the boundary of the contact between the fused trapezium and metacarpal I. This is apparent because its orientation is similar to that of the unfused parts of the suture in a specimen of *M. darwinii* (CORD PZ 4570; pers. obs.). Therefore, it represents further evidence of this fusion in mylodontids, as interpreted for other mylodontid species by most authors (e.g., Lund 1842; Winge 1915; Stock 1925; McDonald 1987), despite exceptions (Owen 1842; Cuenca Anaya 1995). On the distal end of the trapezium-metacarpal I, the articular facet on the dorsoaxial surface in CORD PZ 4586 likely corresponds to a sesamoid on the M. adductor digiti I longus tendon.

On metacarpal IV, the articular facets for the sesamoid bones of CORD PZ 4586 indicate the sesamoids were not fused to the metacarpal, as in the *C. cuvieri* specimens described by Winge (1915), but unlike the *S. leptocephalum* specimens described in the same work (Winge 1915). The lack of an articular facet for the axial sesamoid on the metacarpal IV of CORD PZ 4464 and the presence in the same region of a bulge suggest fusion of the metacarpal IV to the axial sesamoid. Fusion between proximal and intermediate phalanges in the digit I of the manus has been suggested for *V. bucklandi* by Cartelle et al. (2009) and previously for *Paramylodon harlani* by Stock (1925). These hypotheses are likely incorrect, because the first digit has no more than two phalanges (including the ungual) in other mammals (Webb 1989) and most other tetrapods (Noble 1931; Romer 1956). When a single non-ungual phalanx is known, as in many specimens of *Scelidotherium* (and no evidence of fusion is present, as in CORD PZ 4464 and 4586), the most parsimonious interpretation is to infer loss of the ungual phalanx, rather to infer fusion between both phalanges and then loss of the ungual process in the distal one. More assumptions are required to suppose a fused neomorphic intermediate phalanx is present. Phalanges III-1 and III-2 likely did not fuse in CORD PZ 4586, given that the abaxial palmar processes of both phalanges are closer together in that specimen than in CORD PZ 4464. This suggests the former specimen departs in this feature from *V. bucklandi* (Winge 1915; Cartelle et al. 2009). On the distal element of digit IV in CORD PZ 4464, the prominence on the dorsal surface closely resembles the

extensor process of a distal phalanx more than any other feature on the dorsal surface of other intermediate phalanges. This suggests that the distalmost phalanx of digit IV of the manus formed through a fusion of the originally intermediate and distal phalanges, resembling the condition suggested for *C. cuvieri* by Winge (1915), and differing from the unfused condition of *C. tarijensis* (Cuenca Anaya 1995).

Conclusions

Currently reviewed evidence supports referral of the presently described specimens CORD PZ 4464, 4586, and 11293 to the genus *Scelidotherium*. Variation is present within the genus *Scelidotherium*, as indicated by the differences seen in the material from Rosario de la Frontera and the Province of Córdoba. The anatomy of the sloth manus provides evidence useful for understanding the relationships of scelidotheriines, as it does with mylodontines. These characters include a metacarpal II wider at the proximal end than 55% its proximodistal length, a sharp ridge on the articular surface for metacarpal II in the trapezoid, an articular facet for metacarpal II on the magnum largely on the dorsal region of the bone, a notch on the axial border of the distal articular surface of metacarpal II, and a markedly flattened distal phalanx in digit II of the manus, which indicate a closer relationship between the genera *Scelidotherium* and *Catonyx* than with *Valgipes*. The proposed phylogenetic scheme coming from inclusion of data from the structure of the skeleton of the manus only applies to the genera *Scelidotherium*, *Catonyx*, and *Valgipes*, and the species *Pr. gracillimus*. The position of the other species of the genus *Proscelidodon* is however less certain, probably in connection with their less well-known skeleton of the manus.

Acknowledgments We thank R. Leguizamón, D. Álvarez, and J. Di Ronco for the fieldwork and preparation of CORD PZ 4586, K. L. Hansen for information on Lund's collection in Copenhagen, M. Sosa for the drawings, and D. Peters for help with the English style. We thank F. Pujos, E. Amson, and two anonymous reviewers for comments to previous versions of this manuscript that helped improve its quality. We thank the Willi Hennig Society for the free availability of the phylogenetic inference software TNT, CONICET for the postdoctoral fellowship to J. A. H., and the doctoral fellowships to G. L. N. and J. M. K. Funding for this research was provided by the SeCyT-Universidad Nacional de Córdoba grant 05/I780 to A.A.T.

Availability of Data and Material All data generated or analyzed during this study are included in this published article [and its supplementary information files].

Code Availability Not applicable.

Author's Contributions G.L.N. and J.A.H. conceived and designed the project. A.A. T. and J.M.K. found and prepared the fossil material of *Scelidotherium*. G.L.N, J.A.H., A.R.M-B., and H.G.M. collected the *Scelidotherium* data. G.L.N and J.A.H. analyzed the data and drafted the manuscript. M.N.F. and F.M.R. photographed the materials. J.A.H. made all figures, tables, and supplementary files. All authors edited the manuscript and gave final approval for publication.

Funding SeCyT-Universidad Nacional de Córdoba grant 05/I780 to A.A.T.

Compliance with Ethical Standards

Competing Interests The authors declare that they have no competing interests.

Ethics Approval Not applicable.

Consent to Participate Not applicable.

Consent for Publication Not applicable

References

Ameghino F (1887) Enumeración sistemática de las especies de mamíferos fósiles coleccionadas por Carlos Ameghino en los terrenos eocenos de la Patagonia austral y depositadas en el Museo de La Plata. Bol Mus La Plata 1:5-26

Ameghino F (1888) Rápidas diagnosis de algunos mamíferos fósiles nuevos de la República Argentina. PE Coni e Hijos, Buenos Aires

Ameghino F (1891) Mamíferos y aves fósiles argentinas. Especies nuevas, adiciones y correcciones. Rev Argent Hist Nat 1:240-259

Ameghino F (1904) Nuevas especies de mamíferos cretáceos y terciarios de la República Argentina. An Soc Cient Argent 56:3-142

Ameghino F (1908) Las formaciones sedimentarias de la región litoral de Mar del Plata y Chapadmalal. An Mus Nac Buenos Aires, Serie III 10:343-428

Amson E, Muizon C de, Gaudin TJ (2017) A reappraisal of the phylogeny of the Megatheria (Mammalia: Tardigrada), with an emphasis on the relationships of the Thalassocninae, the marine sloths. Zool J Linnean Soc 179:217-236. https://doi.org/10.1111/zoj.12450

Anthony R (1909) Recherches anatomiques sur les Bradypes arboricoles. Le squelette du paresseux à collier; ses rapports morphologiques avec celui des autres Bradypes. Ann Sci Nat Zool, Neuvième Serie 9:157-285

Aramayo SA (1988) Nuevos restos de *Proscelidodon* sp. (Edentata, Mylodontidae) del yacimiento de Monte Hermoso (Plioceno inferior a medio) Provincia de Buenos Aires, Argentina. Estudio morfológico funcional. In: Actas Segundas Jornadas Geológicas Bonaerenses, Bahía Blanca, Argentina, May 26–29, 1988. Comisión de Investigaciones Científicas (ed), Provincia de Buenos Aires, Argentina, pp 99-107

Bordas AF (1935) Observaciones sobre los géneros "*Scelidodon*" Ameghino y "*Proscelidodon*" n. g. Physis 11:484-491

Boscaini A, Pujos F, Gaudin TJ (2019) A reappraisal of the phylogeny of Mylodontidae (Mammalia, Xenarthra) and the divergence of mylodontine and lestodontine sloths. Zool Scr 48(6):691-710. https://doi.org/10.1111/zsc.12376

Burmeister H (1881) Bericht über ein Skelet von *Scelidotherium leptocephalum*. Monatsber K Preuss Akad Wiss Berl 46:374-380

Cartelle C, De Iuliis G, Lopes-Ferreira R (2009) Systematic revision of tropical Brazilian scelidotheriine sloths (Xenarthra, Mylodontoidea). J Vertebr Paleontol 29:555-566. https://doi.org/10.1671/039.029.0231

Corona A (2012) Los Scelidotheriinae (Xenarthra: Mylodontidae) de Uruguay: sistemática, distribución estratigráfica y cronología. MS

Thesis, Facultad de Ciencias, Universidad de la República, Montevideo

Corona A, Perea D, McDonald HG (2013) *Catonyx cuvieri* (Xenarthra, Mylodontidae, Scelidotheriinae) from the late Pleistocene of Uruguay, with comments regarding the systematics of the subfamily. J Vertebr Paleontol 33(5):1214-1225. https://doi.org/10.1080/02724634.2013.764311

Cuenca Anaya J (1995) El aparato locomotor de los escelidoterios (Edentata, Mammalia) y su paleobiología. Adjuntament de Valencia, Valencia

Cuvier G (1796) Notice sur le squelette d'une très grande espèce de quadrupède inconnue jusqu'à présent, trouvé au Paraguay, et déposé au cabinet d'Histoire naturelle de Madrid. Mag Encycl 1: 303-310

Delsuc F, Kuch M, Gibb GC, Karpinski E, Hackenberger D, Szpak P, Martínez JG, Mead JI, McDonald HG, MacPhee RDE, Billet G (2019) Ancient mitogenomes reveal the evolutionary history and biogeography of sloths. Curr Biol 29:2031-2042. https://doi.org/10.1016/j.cub.2019.05.043

Desmarest MAG (1822) Mammalogie ou Description des Espèces de Mammifères. Seconde Partie. Imprimeur Libraire rue des Poitevins, Paris

Esteban GI, Abdala F, Nasif N (1992) Nuevos restos de *Scelidotherium* (Edentata) de Rosario de La Frontera, provincia de Salta, Argentina. Consideraciones sistemáticas basadas en aspectos morfológicos del carpo. Bol R Soc Esp Hist Nat (Secc Geol) 87:24-35

Farris JS (1990) Phenetics in camouflage. Cladistics 6(1):91-100. https://doi.org/10.1111/j.1096-0031.1990.tb00528.x

Gaudin TJ (2004) Phylogenetic relationships among sloths (Mammalia, Xenarthra, Tardigrada): the craniodental evidence. Zool J Linnean Soc 140:255-305. https://doi.org/10.1111/j.1096-3642.2003.00100.x

Gervais H, Ameghino F (1880) Los Mamíferos de la América Meridional. Igon Hermanos, Buenos Aires

Gervais P (1855) Recherches sur les mammifères fossiles de l'Amérique méridionale. Ann Sci Nat Zool 3:330-338

Gervais P (1874) *Lestodon trigonidens* et *Valgipes deformis*. J Zool 3: 162-164

Gill T (1872) Arrangements of the families of mammals, with analytical tables. Smithson Misc Collect 11:1-98. https://doi.org/10.5962/bhl.title.14607

Goloboff PA, Catalano SA (2016) TNT version 1.5, including a full implementation of phylogenetic morphometrics. Cladistics 32:221-238. https://doi.org/10.1111/cla.12160

Goloboff PA, Farris JS, Nixon KC (2003) T.N.T.: Tree Analysis Using New Technology. Fundación Miguel Lillo Web. http://www.lillo.org.ar/phylogeny/tnt/. Accessed 30 October 2018

Goloboff P, Mattoni C, Quinteros S (2006) Continuous characters analyzed as such. Cladistics 22:589-601. https://doi.org/10.1111/j.1096-0031.2006.00122.x

Haro JA, Tauber AA, Krapovickas JM (2016) The manus of *Mylodon darwinii* Owen (Tardigrada, Mylodontidae) and its phylogenetic implications. J Vertebr Paleontol 36:e1188824. https://doi.org/10.1080/02724634.2016.1188824

Haro JA, Tauber AA, Krapovickas JM (2017) Thoracic member (pectoral girdle and forelimb) bones of *Mylodon darwinii* Owen (Xenarthra, Mylodontidae) from the late Pleistocene of central Argentina and their phylogenetic implications. Paläontol Z 91:439-457. https://doi.org/10.1007/s12542-017-0350-z

Hay OP (1919) Descriptions of some mammalian and fish remains from Florida of probably Pleistocene age. Proc US Natl Mus 56:103-112. https://doi.org/10.5479/si.00963801.56-2291.103

Harris JD (2004) Confusing dinosaurs with mammals: tetrapod phylogenetics and anatomical terminology in the world of homology. Anat Rec 281A(2):1240-1246. https://doi.org/10.1002/ar.a.20078

Hirschfeld SE (1985) Ground sloths from the Friasian La Venta Fauna, with additions to the pre-Friasian Coyaima Fauna of Colombia, South America. Univ Calif Publ Geol Sci 128:1-91

Illiger JKW (1811) Prodromus systematis mammalium et avium; additis terminis zoographicis utriusque classis, eorumque versione Germanica. Salfeld, Berlin. https://doi.org/10.5962/bhl.title.106965

International Committee on Veterinary Gross Anatomical Nomenclature (2005) Nomina Anatomica Veterinaria. 5th edn. ICVGAN Editorial Committee, Hannover, Columbia, Ghent, Sapporo

Kraglievich L (1923) Descripción comparada de los cráneos de *Scelidodon rothi* Ameghino y *Scelidotherium parodii* n. sp. procedentes del horizonte "chapadmalense." An Mus Nac Hist Nat "Bernardino Rivadavia" 33:57-103

Krapovickas JM, Tauber AA, Haro JA (2017) Quaternary biostratigraphy and biogeography of mountain region of Córdoba, Argentina. Geobios 50:211-236. https://doi.org/10.1016/j.geobios.2017.03.001

Latham J, Davies H (1795) Faunula indica. Appendix to Forster JR, Zoologia Indica. Editorial Secunda. Gebauer, Halle an der Saale

Leguizamón R, Álvarez D, Di Ronco J (2000) Hallazgo de un ejemplar de *Scelidotherium* (Tardigrada; Mylodontidae-Scelidotheriinae) en la localidad de Noetinger, este de la provincia de Córdoba, Argentina. Ameghiniana 37(4, Supplement):10R

Lund PW (1839a) Extrait d'une lettre de M. Lund, écrite de Lagoa Santa (Brésil), le 5 novembre 1838, et donnant un aperçu des espèces de mammifères fossiles qu'il a découvertes au Brésil. C R Acad Sci 8: 570-577

Lund PW (1839b) Coup d'œil sur les espèces éteintes de mammifères du Brésil; extrait de quelques mémoires présentés à l'Académie royal des Sciences de Copenhague. Ann Sci Nat Zool 11:214-234

Lund PW (1842) Blik paa Brasiliens Dyreverden før sidste Jordomvæltning. Fjerde Afhandling: Fortsættelse af Pattedyrene. K Dan Vidensk Selsk Naturvidensk Math Afh 9:137-208

Lydekker R (1886) Description of three species of *Scelidotherium*. Proc Zool Soc London 32:491-498

Lydekker R (1894) The extinct edentates of Argentina. An Mus Lą Platą Paleontol Arg 3:1-118 + Pl. I-LXI

McAfee RK (2016) Description of new postcranial elements of *Mylodon darwinii* Owen 1839 (Mammalia: Pilosa: Mylodontinae), and functional morphology of the forelimb. Ameghiniana 53:418-443. https://doi.org/10.5710/AMGH.24.02.2016.2950

McDonald HG (1987) A systematic review of the Plio-Pleistocene scelidotherine ground sloths (Mammalia: Xenarthra: Mylodontidae). PhD dissertation, University of Toronto, Toronto

McDonald HG, Perea D (2002) The large scelidothere *Catonyx tarijensis* (Xenarthra, Mylodontidae) from the Pleistocene of Uruguay. J Vertebr Paleontol 22:677-683. https://doi.org/10.1671/0272-4634(2002)022[0677:TLSCTX]2.0.CO;2

Miño-Boilini ÁR (2012) Sistemática y evolución de los Scelidotheriinae (Xenarthra, Mylodontidae) cuaternarios de la Argentina. Importancia bioestratigráfica, paleobiogeográfica y paleoambiental. PhD dissertation, Universidad Nacional de La Plata, La Plata

Miño-Boilini ÁR (2016) Additions to the knowledge of the ground sloth *Catonyx tarijensis* (Xenarthra, Pilosa) in the Pleistocene of Argentina. Paläontol Z 90:173-183. https://doi.org/10.1007/s12542-015-0280-6

Miño-Boilini ÁR, Carlini AA, Scillato-Yané GJ (2014) Revisión sistemática y taxonómica del género *Scelidotherium* Owen, 1839 (Xenarthra, Phyllophaga, Mylodontidae). Rev Bras Paleontol 17: 43-58. https://doi.org/10.4072/rbp.2014.1.05

Noble GK (1931) The Biology of the Amphibia. McGraw-Hill, New York and London

Ortega E (1967) Descripción de los restos de un Scelidotheriinae (Edentata, Mylodontidae) de Edad Huayqueriense. Algunas consideraciones en torno a la filogenia de los Scelidotheriinae. Ameghiniana 5:109-118

Owen R (1839) Part I. Fossil Mammalia. In: Darwin C (ed) The Zoology of the Voyage of HMS Beagle. Smith, Elder and Co., London, pp 13-111

Owen R (1842) Description of the skeleton of an extinct gigantic sloth, *Mylodon robustus*, Owen, with observations on the osteology, natural affinities, and probable habits of the megatherioid quadrupeds in general. R and JE Taylor, London

Owen R (1857) On the scelidothere (*Scelidotherium leptocephalum*, Owen), a large extinct terrestrial sloth. Proc R Soc Lond 8:312-314. https://doi.org/10.1098/rspl.1856.0078

Peters W (1858) Charakterist eines neuen zweizehigen Faulthiers. Monatsber k preuss Akad Wiss Berl 1858:128

Presslee S, Slater GJ, Pujos, F, Forasiepi AM, Fischer R, Molloy K, Mackie M, Olsen JV, Kramarz A, Taglioretti M, Scaglia F, Lezcano M, Lanata JL, Southon J, Feranec R, Bloch J, Hajduk A, Martin FM, Salas Gismondi R, Reguero M, De Muizon C, Greenwood A, Chait BT, Penkman K, Collins M, MacPhee RDE (2019) Palaeoproteomics resolves sloth relationships. Nat Ecol & Evol 3:1121-1130. https://doi.org/10.1038/s41559-019-0909-z

Pujos F (2000) *Scelidodon chiliensis* (Mammalia, Xenarthra) du Pléistocène terminal de "Pampa de los Fósiles" (Nord-Pérou). Quaternaire 11:197-206. https://doi.org/10.3406/quate.2000.1669

Romer AS (1956) Osteology of the Reptiles. University of Chicago Press, Chicago

Rovereto C (1914) Los estratos araucanos y sus fósiles. An Mus Nac Hist Nat Buenos Aires 25:1-247

Schulthess B (1920) Beiträge zur kenntnis der Xenarthra auf grund der «Santiago Roth'schen Sammlung» des Zoologischen museums der Universität Zürich. Mém Soc Paléontol Suisse 44:1-119

Scillato-Yané GJ, Carlini AA (1998) Nuevos Xenarthra del Friasense (Mioceno medio) de Argentina. Stud Geol Salmant 34:43-67

Scott WB (1904) Mammalia of the Santa Cruz beds, part I, Edentata. Rep Princet Univ Exped Patagon, 1896–1899 5:161-364

Sefve I (1915) *Scelidotherium*-Reste aus Ulloma, Bolivia. Bull Geol Inst Univ Upsala 13:61-92

Stock C (1925) Cenozoic Gravigrade Edentates of Western North America with Special Reference to the Pleistocene Megalonychinae and Mylodontidae of Rancho La Brea. Carnegie Institute of Washington, Washington

Taglioretti M, Miño-Boilini ÁR, Scaglia F, Dondas A (2014) Presencia de *Proscelidodon patrius* (Xenarthra, Scelidotheriinae) en la Formación Chapadmalal (Plioceno superior), Mar del Plata, Buenos Aires, Argentina: implicancias bioestratigráficas. Ameghiniana 51:420-427. https://doi.org/10.5710/AMGH.04.08.2014.2715

Tschopp E, Mateus O, Benson RBJ (2015) A specimen-level phylogenetic analysis and taxonomic revision of Diplodocidae (Dinosauria, Sauropoda). PeerJ 3:e857. https://doi.org/10.7717/peerj.857

Vrana P, Wheeler W (1992) Individual organisms as terminal entities: laying the species problem to rest. Cladistics 8:67-72. https://doi.org/10.1111/j.1096-0031.1992.tb00051.x

Webb SD (1989) Osteology and relationship of *Thinobadistes segnis*, the first mylodont sloth in North America. In: Redford KH, Eisenberg JF (eds) Advances in Neotropical Mammalogy. Sandhill Crane Press, Gainesville, pp 496-532

Winge H (1915) Jordfunde og nulevende Gumlere (Edentata) fra Lagoa Santa, Minas Gerais, Brasilien. E Mus Lundii, Copenhagen 3:1-321

Yates AM (2003) The species taxonomy of the sauropodomorph dinosaurs from the Löwenstein Formation (Norian, Late Triassic) of Germany. Palaeontology 46:317-337. https://doi.org/10.1111/j.0031-0239.2003.00301.x